endothelial cells,[47] whereas others show that VE-cadherin$^+$ endothelial cells derived from mouse ESCs generate primitive and definitive hematopoietic cells.[48] Here, we demonstrate that primitive and definitive hematopoietic cells are, at least in part, generated from a subset of endothelial cells in primates. Because primitive hematopoiesis occurs only in the yolk sac, we hypothesized that ESC-derived VE-cadherin$^+$CD45$^-$ endothelial cells are equivalent to those in yolk sac blood islands and possibly in the AGM region in vivo.

VE-cadherin is a specific endothelial lineage marker,[15,16,26,37] whereas CD45 is widely accepted as a specific hematopoietic lineage marker except in erythroid and megakaryocytic lineage cells. Based on reports that VE-cadherin$^+$CD45$^+$ intermediate cells exist in mouse embryos,[49,50] we isolated VE-cadherin$^+$CD45$^-$ cells as definitive endothelial, but not hematopoietic, cells. In addition, our immunochemistry and FACS analyses demonstrated that VE-cadherin$^+$CD45$^-$ cells on day 10 of culture coexpress other endothelial markers, such as CD31, CD34, VEGFR-2, and eNOS, and take up Ac-LDL but that they lack mature endothelial properties, including VWF expression (Figure 1D-J). These results are consistent with the established multiparameter criteria for defining endothelial cells.[45,51] Furthermore, VE-cadherin$^+$CD45$^-$ cells are devoid of hematopoietic specific marker expression, such as hemoglobin, CD45, and CD41a. Thus, the VE-cadherin$^+$CD45$^-$ cells in this study are confirmed as endothelial, albeit immature, cells.

Studies show that β-globin is the most specific type of globin gene for the identification of definitive erythrocytes during human embryogenesis and primate ESC differentiation.[4,25,29,30,34] In our experiments, VE-cadherin$^+$CD45$^-$ cells initially produced larger, nucleated erythrocytes almost with no β-globin expression and later generated smaller, partly enucleated, erythrocytes expressing β-globin (Figures 2C-D, P, 3). This result is morphologically supported by the finding that human ESC-derived erythroblasts devoid of β-globin expression are megaloblastic and similar to primitive erythroid cells found in 4- to 5-week-old human embryos.[44] On the other hand, our results showed that the high proportion of β-globin$^+$ cells on day 10 + 30 also expressed embryonic globins (ε and ζ). This is consistent with previous reports that the embryonic globins and β-globin are expressed in early definitive hematopoietic cells.[29,30] Hence, VE-cadherin$^+$CD45$^-$ endothelial cells isolated on day 10 generated primitive and definitive erythrocytes sequentially.

Clonal analysis disclosed that 1.1% of the single VE-cadherin$^+$CD45$^-$ cells yielded endothelial and hematopoietic cells (Figure S1). Our results are in agreement with previous data,[45] and the characteristics of endothelial cells isolated by both groups are similar. Given that VE-cadherin$^-$CD45$^-$ cells almost never generated endothelial colonies, even under endothelial culture conditions (Figure 2R), we suggest that bipotential cells among the VE-cadherin$^+$CD45$^-$ population are not the contaminating cells during cell sorting.

α4-Integrin is a marker of the hemogenic endothelial cells in primates

The differences between hemogenic and nonhemogenic endothelial cells and how a subset of endothelial cells acquires hemogenic capacity during early embryogenesis in primates remain unclear. Here, we used α4-integrin as a candidate marker of hemogenic endothelial cells. To our knowledge, there are no reports on the expression or function of α4-integrin during early primate embryogenesis. Developmentally, in mice, α4-integrin is expressed on yolk sac blood islands and all hematopoietic cells in the fetal liver.[52,53] It is essential for the maintenance of efficient development of multilineage progenitors in the fetal liver[54] and is a marker of the earliest precursor of the hematopoietic cell lineage from endothelial progenitors in vivo and in vitro.[26] We show that the α4-integrin$^+$, not the α4-integrin$^-$ subpopulation among ESC-derived endothelial cells, yields hematopoietic cells. Except for the generation of primitive hematopoiesis, this is consistent with previous findings in mice.[26] In our study, α4-integrin$^+$ hemogenic endothelial cells generated primitive and definitive hematopoietic cells, as confirmed by immunostaining of erythroid cells/colonies (Figures 6, S2), though it remains to be clarified whether primitive and definitive hematopoiesis have common precursors.

In human embryos, yolk sac blood islands are observed from gestational days 16 to 24, and intraaortic hematopoietic cell clusters are observed in the AGM region from days 27 to 40.[55,56] The frequency of hemogenic endothelial cells in vivo reflects the actual blood-forming activity of these hematopoietic tissues as a function of developmental age.[12] Interestingly, α4-integrin$^+$ endothelial cells were detected for a limited period of time in this study (Figure 4), but primitive and definitive hematopoietic cells emerged sequentially, suggesting that precursors of primitive and definitive hematopoiesis arise simultaneously but that the definitive precursors required a maturation phase (on OP9) before they differentiated into hematopoietic cells. This may recapitulate the hemogenic activity of endothelial cells in and temporal lag of hematopoiesis between yolk sac blood islands and the AGM region in vivo.

The transcriptional factor *Runx1* is required for definitive hematopoiesis.[40,41] *Runx1* is expressed in endothelial cells where definitive hematopoietic cells emerge, specifically the yolk sac, vitelline and umbilical arteries, and ventral wall of the dorsal aorta in the AGM region but not in endothelial cells elsewhere in mouse embryos.[57] In addition, *Runx1* is reportedly required for the formation of intraaortic hematopoietic clusters and the emergence of hematopoietic stem cells.[57-59] Our RT-PCR data show that *RUNX1* is expressed in the hemogenic α4-integrin$^+$ subpopulation, but not the nonhemogenic α4-integrin$^-$ subpopulation, among ESC-derived endothelial cells (Figure 5J). *RUNX1* is additionally expressed in the VE-cadherin$^-$α4-integrin$^+$ population generating mainly primitive erythrocytes, consistent with the finding that primitive erythrocytes in the yolk sac express *Runx1* 8 days after coitus in mice.[57]

Based on the results from this study, we propose a model of primitive/definitive hematopoietic and endothelial lineage development from primate ESCs (Figure 7). We suggest that VE-cadherin$^-$CD45$^-$α4-integrin$^+$ and VE-cadherin$^+$CD45$^-$α4-integrin$^+$ cells contain a subset with hemogenic capacity and that these are primary sources for primitive and definitive hematopoiesis, respectively. Moreover, we hypothesize that in primates,

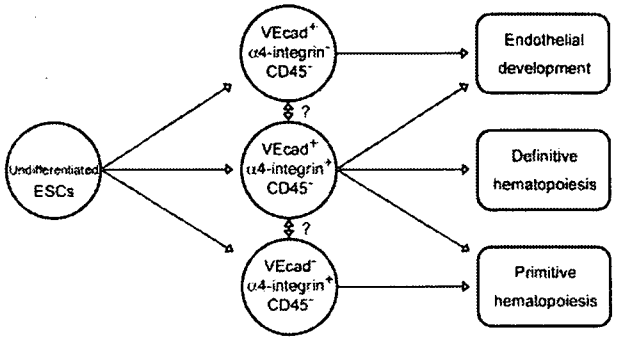

Figure 7. Schematic representation of the differentiation pathway from ESCs into endothelial or primitive and definitive hematopoietic cell lineages on coculture with OP9 cells.

hemogenic endothelial cells are located in the yolk sac and in the AGM region, generate primitive and definitive hematopoietic cells, and are marked by the temporal expression of α4-integrin. The function of α4-integrin during hematopoietic development remains to be elucidated.

In conclusion, we have successfully induced the differentiation of nonhuman primate ESCs into hemogenic endothelial cells, which in turn gave rise to primitive and definitive hematopoietic cells with the OP9 coculture system. Hemogenic activity exclusively resides in the α4-integrin$^+$ subpopulation among endothelial cells. Our culture system should provide an alternative, powerful tool for understanding early hematopoietic development during primate embryogenesis, such as the processes triggering transition from endothelial cells to hematopoietic cells in the yolk sac and the AGM region or the initial emergence of hematopoietic stem cells.

Acknowledgments

This work was supported by grants from Science Research on Priority Areas; Creative Science Research; the Japan Society for the Promotion of Science; the Ministry of Education, Culture, Sports, Science and Technology; and Tanabe Seiyaku (Osaka, Japan) for help with primate ESC preparation.

Authorship

Contribution: G.S. performed all the experiments and wrote the manuscript. K.U. contributed to the study design, data analysis, and writing of the manuscript. T.H. contributed to the study design, data analysis, and writing of the manuscript. M.A. contributed to the study design, writing of the manuscript, and interpretation of the results. A.N. contributed to the study design and developed a method for colony-forming assays. F.M. supervised the flow cytometric analysis. H.S. supervised the culture of primate embryonic stem cells. H.Y.L. contributed vital antibodies. D.H.K.C. contributed vital antibodies and revised the manuscript. R.T. supervised the culture of primate embryonic stem cells. M.S. contributed vital antibodies. N.N. contributed to the study design and supervised the culture of primate embryonic stem cells. T.N. supervised the study and contributed to the study design and to the writing and revision of the manuscript.

Conflict-of-interest disclosure: The authors declare no competing financial interests.

Correspondence: Tatsutoshi Nakahata, Department of Pediatrics, Graduate School of Medicine, Kyoto University, 54 Kawahara-cho, Shogoin, Sakyo-ku, Kyoto 606-8507, Japan; e-mail: tnakaha@kuhp.kyoto-u.ac.jp.

References

1. Palis J, Yoder MC. Yolk-sac hematopoiesis: the first blood cells of mouse and man. Exp Hematol. 2001;29:927-936.
2. Palis J, Robertson S, Kennedy M, Wall C, Keller G. Development of erythroid and myeloid progenitors in the yolk sac and embryo proper of the mouse. Development. 1999;126:5073-5084.
3. Stamatoyannopoulos G, Constantoulakis P, Brice M, Kurachi S, Papayannopoulou T. Coexpression of embryonic, fetal, and adult globins in erythroid cells of human embryos: relevance to the cell-lineage models of globin switching. Dev Biol. 1987;123:191-197.
4. Peschle C, Mavilio F, Care A, et al. Haemoglobin switching in human embryos: asynchrony of zeta → alpha and epsilon → gamma-globin switches in primitive and definite erythropoietic lineage. Nature. 1985;313:235-238.
5. Sabin F. Studies on the origin of blood vessels and of red corpuscles as seen in the living blastoderm of the chick during the second day of incubation. Contributions to Embryology. 1920;9:213-262.
6. Murray P. The development in vitro of the blood of the early chick embryo. Proc R Soc London. 1932;11:497-521.
7. Shalaby F, Ho J, Stanford WL, et al. A requirement for Flk1 in primitive and definitive hematopoiesis and vasculogenesis. Cell. 1997;89:981-990.
8. Shalaby F, Rossant J, Yamaguchi TP, et al. Failure of blood-island formation and vasculogenesis in Flk-1-deficient mice. Nature. 1995;376:62-66.
9. Choi K, Kennedy M, Kazarov A, Papadimitriou JC, Keller G. A common precursor for hematopoietic and endothelial cells. Development. 1998; 125:725-732.
10. Sugiyama D, Ogawa M, Hirose I, Jaffredo T, Arai K, Tsuji K. Erythropoiesis from acetyl LDL incorporating endothelial cells at the preliver stage. Blood. 2003;101:4733-4738.
11. de Bruijn MF, Ma X, Robin C, Ottersbach K, Sanchez MJ, Dzierzak E. Hematopoietic stem cells localize to the endothelial cell layer in the midgestation mouse aorta. Immunity. 2002;16: 673-683.
12. Oberlin E, Tavian M, Blazsek I, Peault B. Blood-forming potential of vascular endothelium in the human embryo. Development. 2002;129:4147-4157.
13. Jaffredo T, Gautier R, Brajeul V, Dieterlen-Lievre F. Tracing the progeny of the aortic hemangioblast in the avian embryo. Dev Biol. 2000;224: 204-214.
14. Jaffredo T, Gautier R, Eichmann A, Dieterlen-Lievre F. Intraaortic hemopoietic cells are derived from endothelial cells during ontogeny. Development. 1998;125:4575-4583.
15. Nishikawa SI, Nishikawa S, Kawamoto H, et al. In vitro generation of lymphohematopoietic cells from endothelial cells purified from murine embryos. Immunity. 1998;8:761-769.
16. Nishikawa SI, Nishikawa S, Hirashima M, Matsuyoshi N, Kodama H. Progressive lineage analysis by cell sorting and culture identifies FLK1+VE-cadherin+ cells at a diverging point of endothelial and hemopoietic lineages. Development. 1998; 125:1747-1757.
17. Nishikawa SI. A complex linkage in the developmental pathway of endothelial and hematopoietic cells. Curr Opin Cell Biol. 2001;13:673-678.
18. Smith RA, Glomski CA. "Hemogenic endothelium" of the embryonic aorta: does it exist? Dev Comp Immunol. 1982;6:359-368.
19. Suemori H, Tada T, Torii R, et al. Establishment of embryonic stem cell lines from cynomolgus monkey blastocysts produced by IVF or ICSI. Dev Dyn. 2001;222:273-279.
20. Thomson JA, Itskovitz-Eldor J, Shapiro SS, et al. Embryonic stem cell lines derived from human blastocysts. Science. 1998;282:1145-1147.
21. Thomson JA, Kalishman J, Golos TG, Durning M, Harris CP, Hearn JP. Pluripotent cell lines derived from common marmoset (*Callithrix jacchus*) blastocysts. Biol Reprod. 1996;55:254-259.
22. Thomson JA, Kalishman J, Golos TG, et al. Isolation of a primate embryonic stem cell line. Proc Natl Acad Sci U S A. 1995;92:7844-7848.
23. Umeda K, Heike T, Yoshimoto M, et al. Identification and characterization of hemoangiogenic progenitors during cynomolgus monkey embryonic stem cell differentiation. Stem Cells. 2006;24: 1348-1358.
24. Umeda K, Heike T, Yoshimoto M, et al. Development of primitive and definitive hematopoiesis from nonhuman primate embryonic stem cells in vitro. Development. 2004;131:1869-1879.
25. Umeda K, Heike T, Nakata-Hizume M, et al. Sequential analysis of α- and β-globin gene expression during erythropoietic differentiation from primate embryonic stem cells. Stem Cells. Prepublished on August 3, 2006, as DOI 10.1634/stemcells-2006-0199.
26. Ogawa M, Kizumoto M, Nishikawa S, Fujimoto T, Kodama H, Nishikawa SI. Expression of α4-integrin defines the earliest precursor of hematopoietic cell lineage diverged from endothelial cells. Blood. 1999;93:1168-1177.
27. Furuya M, Yasuchika K, Mizutani K, Yoshimura Y, Nakatsuji N, Suemori H. Electroporation of cynomolgus monkey embryonic stem cells. Genesis. 2003;37:180-187.
28. Sawano A, Iwai S, Sakurai Y, et al. Flt-1, vascular endothelial growth factor receptor 1, is a novel cell surface marker for the lineage of monocyte-macrophages in humans. Blood. 2001;97:785-791.
29. Luo HY, Liang XL, Frye C, et al. Embryonic hemoglobins are expressed in definitive cells. Blood. 1999;94:359-361.
30. Chui DH, Mentzer WC, Patterson M, et al. Human embryonic zeta-globin chains in fetal and newborn blood. Blood. 1989;74:1409-1414.
31. Suwabe N, Takahashi S, Nakano T, Yamamoto M. GATA-1 regulates growth and differentiation of definitive erythroid lineage cells during in vitro ES cell differentiation. Blood. 1998;92:4108-4118.
32. Tajima S, Tsuji K, Ebihara Y, et al. Analysis of interleukin 6 receptor and gp130 expressions and proliferative capability of human CD34+ cells. J Exp Med. 1996;184:1357-1364.
33. Nakahata T, Ogawa M. Hemopoietic colony-forming cells in umbilical cord blood with extensive capability to generate mono- and multipotential hemopoietic progenitors. J Clin Invest. 1982;70: 1324-1328.
34. Zambidis ET, Peault B, Park TS, Bunz F, Civin CI.

Hematopoietic differentiation of human embryonic stem cells progresses through sequential hematoendothelial, primitive, and definitive stages resembling human yolk sac development. Blood. 2005;106:860-870.

35. Lampugnani MG, Resnati M, Raiteri M, et al. A novel endothelial-specific membrane protein is a marker of cell-cell contacts. J Cell Biol. 1992;118: 1511-1522.
36. Breier G, Breviario F, Caveda L, et al. Molecular cloning and expression of murine vascular endothelial-cadherin in early stage development of cardiovascular system. Blood. 1996;87:630-641.
37. Fraser ST, Ogawa M, Yu RT, Nishikawa S, Yoder MC, Nishikawa S. Definitive hematopoietic commitment within the embryonic vascular endothelial-cadherin(+) population. Exp Hematol. 2002;30: 1070-1078.
38. Kallianpur AR, Jordan JE, Brandt SJ. The *SCL/TAL-1* gene is expressed in progenitors of both the hematopoietic and vascular systems during embryogenesis. Blood. 1994;83:1200-1208.
39. Tsai FY, Keller G, Kuo FC, et al. An early haematopoietic defect in mice lacking the transcription factor GATA-2. Nature. 1994;371:221-226.
40. Wang Q, Stacy T, Binder M, Marin-Padilla M, Sharpe AH, Speck NA. Disruption of the Cbfa2 gene causes necrosis and hemorrhaging in the central nervous system and blocks definitive hematopoiesis. Proc Natl Acad Sci U S A. 1996;93: 3444-3449.
41. Okuda T, van Deursen J, Hiebert SW, Grosveld G, Downing JR. AML1, the target of multiple chromosomal translocations in human leukemia, is essential for normal fetal liver hematopoiesis. Cell. 1996;84:321-330.
42. Nakano T, Kodama H, Honjo T. In vitro development of primitive and definitive erythrocytes from different precursors. Science. 1996;272:722-724.
43. Vodyanik MA, Bork JA, Thomson JA, Slukvin, II. Human embryonic stem cell-derived CD34+ cells: efficient production in the coculture with OP9 stromal cells and analysis of lymphohematopoietic potential. Blood. 2005;105:617-626.
44. Qiu C, Hanson E, Olivier E, et al. Differentiation of human embryonic stem cells into hematopoietic cells by coculture with human fetal liver cells recapitulates the globin switch that occurs early in development. Exp Hematol. 2005;33:1450-1458.
45. Wang L, Li L, Shojaei F, et al. Endothelial and hematopoietic cell fate of human embryonic stem cells originates from primitive endothelium with hemangioblastic properties. Immunity. 2004;21: 31-41.
46. Kaufman DS, Hanson ET, Lewis RL, Auerbach R, Thomson JA. Hematopoietic colony-forming cells derived from human embryonic stem cells. Proc Natl Acad Sci U S A. 2001;98:10716-10721.
47. Fujimoto T, Ogawa M, Minegishi N, et al. Stepwise divergence of primitive and definitive haematopoietic and endothelial cell lineages during embryonic stem cell differentiation. Genes Cells. 2001;6:1113-1127.
48. Zhang WJ, Park C, Arentson E, Choi K. Modulation of hematopoietic and endothelial cell differentiation from mouse embryonic stem cells by different culture conditions. Blood. 2005;105:111-114.
49. Taoudi S, Morrison AM, Inoue H, Gribi R, Ure J, Medvinsky A. Progressive divergence of definitive haematopoietic stem cells from the endothelial compartment does not depend on contact with the foetal liver. Development. 2005;132:4179-4191.
50. Fraser ST, Ogawa M, Yokomizo T, Ito Y, Nishikawa S, Nishikawa S. Putative intermediate precursor between hematogenic endothelial cells and blood cells in the developing embryo. Dev Growth Differ. 2003;45:63-75.
51. Rafii S, Lyden D. Therapeutic stem and progenitor cell transplantation for organ vascularization and regeneration. Nat Med. 2003;9:702-712.
52. Hamamura K, Matsuda H, Takeuchi Y, Habu S, Yagita H, Okumura K. A critical role of VLA-4 in erythropoiesis in vivo. Blood. 1996;87:2513-2517.
53. Sheppard AM, Onken MD, Rosen GD, Noakes PG, Dean DC. Expanding roles for alpha 4 integrin and its ligands in development. Cell Adhes Commun. 1994;2:27-43.
54. Arroyo AG, Yang JT, Rayburn H, Hynes RO. α4 Integrins regulate the proliferation/differentiation balance of multilineage hematopoietic progenitors in vivo. Immunity. 1999;11:555-566.
55. Tavian M, Peault B. Embryonic development of the human hematopoietic system. Int J Dev Biol. 2005;49:243-250.
56. Tavian M, Hallais MF, Peault B. Emergence of intraembryonic hematopoietic precursors in the pre-liver human embryo. Development. 1999; 126:793-803.
57. North T, Gu TL, Stacy T, et al. Cbfa2 is required for the formation of intra-aortic hematopoietic clusters. Development. 1999;126:2563-2575.
58. North TE, de Bruijn MF, Stacy T, et al. Runx1 expression marks long-term repopulating hematopoietic stem cells in the midgestation mouse embryo. Immunity. 2002;16:661-672.
59. Yokomizo T, Ogawa M, Osato M, et al. Requirement of Runx1/AML1/PEBP2αB for the generation of haematopoietic cells from endothelial cells. Genes Cells. 2001;6:13-23.

The FASEB Journal • Research Communication

Human cord blood CD34$^+$ cells develop into hepatocytes in the livers of NOD/SCID/γ_c^{null} mice through cell fusion

Hisanori Fujino, Hidefumi Hiramatsu, Atsunori Tsuchiya, Akira Niwa, Haruyoshi Noma, Mitsutaka Shiota, Katsutsugu Umeda, Momoko Yoshimoto, Mamoru Ito, Toshio Heike, and Tatsutoshi Nakahata[1]

Department of Pediatrics, Graduate School of Medicine, Kyoto University, Kyoto, Japan; and the Central Institute for Experimental Animals, Kawasaki, Japan

ABSTRACT **Several studies have shown that hepatocytes can be generated from hematopoietic stem cells, but this event is believed to be rare and to require hepatic damage. To investigate this phenomenon in human cells, we used a NOD/SCID/γ_c^{null} (NOG) mouse model that can achieve a tremendously high level of chimerism when transplanted with human hematopoietic cells. Even without hepatotoxic treatment other than irradiation, human albumin and α-1-antitrypsin-positive cells were invariably detected in the livers of NOG mice after i.v. transplantation of human cord blood CD34$^+$ cells. Human albumin was detected in the murine sera, indicating functional maturation of the human hepatocytes. Flow cytometric analysis of recipient liver cells in single-cell suspension demonstrated that human albumin-positive cells were also positive for both murine and human MHC and were negative for human CD45. PCR analysis of recipient livers revealed the expression of a wide variety of human hepatocyte- or cholangiocyte-specific mRNAs. These results show that human CD34$^+$ cells fuse with hepatocytes of NOG mice without liver injury, lose their hematopoietic phenotype, and begin hepatocyte-specific gene transcription. These phenomena were not observed when CD34$^-$ cells were transplanted. Thus, our model revealed a previously unidentified pathway of human hematopoietic stem/progenitor cell differentiation.—Fujino, H., Hiramatsu, H., Tsuchiya, A., Niwa, A., Noma, H., Shiota, M., Umeda, K., Yoshimoto, M., Ito, M., Heike, T., Nakahata, T. Human cord blood CD34$^+$ cells develop into hepatocytes in the livers of NOD/SCID/γ_c^{null} mice through cell fusion. *FASEB J.* 21, 3499–3510 (2007)**

Key Words: liver regeneration · hematopoietic stem/progenitor cell · mature hepatocyte · bone marrow-derived cell

THE LIVER IS AN ORGAN WITH A NATURALLY HIGH regeneration potential. A number of hepatic cell types have been found to have regeneration potential, including liver intrinsic stem/progenitor cells, oval cells, and mature hepatocytes (1). As a general rule, the replication of existing hepatocytes is the quickest and most efficient way to generate hepatocytes for liver regeneration. In contrast, liver regeneration by oval cells takes place only when the replication of mature hepatocytes is delayed or entirely blocked, such as when acute and severe hepatocellular damage has occurred (1).

Recent studies of mice have revealed a new liver-regenerating cell type, namely, bone marrow cells. In 2000, Lagasse *et al.* (2) first showed that i.v. injection of purified bone marrow hematopoietic stem cells (c-kit^{high}Thy^{low}Lin$^-$Sca-1$^+$ cells) into mice with a lethal fumarylacetoacetate hydrolase (FAH) deficiency rescued the recipients by restoring the biochemical function of their livers; on the basis of this, they proposed the notion of "transdifferentiation," or the differentiation of hematopoietic stem cells into nonhematopoietic cells. However, in 2002 this concept of plasticity was challenged by Terada *et al.* (3) and Ying *et al.* (4), when they found that adult stem cells spontaneously fused with embryonic stem cells and took on their characteristics; these authors concluded that "cell fusion" was the mechanism of nonhematopoietic cell generation from hematopoietic cells. Studies in 2003 by Wang *et al.* (5), Vassilopoulos *et al.* (6), and Alvarez-Dolado *et al.* (7) supported the cell fusion hypothesis. However, Jang *et al.* (8) and Harris *et al.* (9) reported in 2004 that hepatocytes that differentiate from bone marrow-derived cells are not the result of cell fusion. In the same year, Willenbring *et al.* (10) and Camargo *et al.* (11) showed that hematopoietic myelomonocytic-committed cells such as macrophages are the major source of hepatocyte fusion partners. Thus, it remains unclear whether transdifferentiation or cell fusion is the main mechanism that generates hepatocytes from hematopoietic cells.

[1] Correspondence: Department of Pediatrics, Graduate School of Medicine, Kyoto University, 54 Kawahara-cho, Shogoin, Sakyo-ku, Kyoto 606-8507, Japan. E-mail: tnakaha@kuhp.kyoto-u.ac.jp

doi: 10.1096/fj.06-6109com

In humans, Alison *et al.* (12) and Theise *et al.* (13) showed that the adult human hematopoietic stem cell population can yield hepatocytes upon instruction by the appropriate environment. Korbling *et al.* (14) showed that hepatocytes are generated from the bone marrow of recipients of sex-mismatched bone marrow transplants at a high frequency that ranges from 4% to 7%. Moreover, Ng *et al.* (15) found that in human liver allografts, although most of the recipient-derived cells showed macrophage/Kupffer cell differentiation, recipient-derived hepatocytes were also present and constituted 0.62% of all the hepatocytes in the recipient.

To examine the mechanisms by which human hematopoietic cells contribute to liver regeneration, the human-to-mouse xenogeneic transplantation model was used. Several reports have shown that when human cord blood (CB) cells (all cells, $CD34^+$ cells, or $CD45^+$ cells) are injected into mice through either the portal vein or the systemic circulation, they can form human hepatocyte-like cells in the murine liver environment (16–23). However, even when there is massive liver damage, the frequency with which this hepatocytic differentiation occurs is low compared to that reported in human-to-human transplantation studies. This low level of efficiency makes it hard to clarify whether transdifferentiation or cell fusion is the primary mechanism that generates hepatocytes from human hematopoietic cells. Many attempts have been made to establish more suitable models but have met with limited success.

We postulated that the failure to achieve substantial hepatic chimerism in standard mouse models is due to *1)* the low frequency of human hematopoietic cells combined with *2)* the intrinsic immune barrier of the murine liver, which will mask the true regenerating potential of human hematopoietic cells. We previously reported that the NOD/SCID/γ_c^{null} mouse model provided far better human hematopoietic stem cell engraftment than did NOD/SCID and NOD/SCID/$\beta 2m^{null}$ mice (24–26). NOD/SCID/γ_c^{null} mice completely lack natural killer (NK) cell activity and have dendritic cell dysfunction (24). Notably, functional human T, NK, and mast cells have been generated and matured from human hematopoietic stem cells in NOD/SCID/γ_c^{null} mice (25, 26).

Here we have used the NOD/SCID/γ_c^{null} mouse model to address questions about the regeneration of the liver from transplanted human hematopoietic stem cells. First, we asked whether human CB $CD34^+$ cells could develop into functional hepatic and cholangitic cells in the murine liver environment. Second, we asked whether the generation of hepatocytes is due to transdifferentiation or cell fusion. Third, we examined the status of human liver-specific gene transcription in the murine liver. Finally, we investigated whether $CD34^-$ cells also have the ability to produce hepatocytes. Our model proved suitable for answering these questions and revealed a previously unidentified pathway of human $CD34^+$ cell differentiation under steady-state conditions.

MATERIALS AND METHODS

Mice

NOD/SCID/γ_c^{null} mice were generated at the Central Institute for Experimental Animals (Kawasaki, Japan), shipped to the animal facility of Kyoto University (Kyoto, Japan), and handled with humane care under pathogen-free conditions. All experiments in this study were performed in accordance with the Animal Protection Guidelines of Kyoto University.

Cell preparation and transplantation protocol

Human CB $CD34^+$ cells were purified using a described method (25). Briefly, after we obtained informed consent from the donors parents, we collected mononuclear cells from human CB by Ficoll-Hypaque (Pharmacia, Uppsala, Sweden) density gradient centrifugation. The $CD34^+$ fraction was then isolated by using auto-MACS (Miltenyi Biotec GmbH, Bergisch Gladbach, Germany) with the "posseld2" program according to the manufacturer's recommendations. The "depl 05" and "possel" programs were added to get the $CD34^-$ fraction and the $CD34^-CD14^{+/-}$ fraction, respectively; this yielded highly pure populations. Eight- to 12-wk-old NOD/SCID/γ_c^{null} mice were irradiated with 240cGy, and human CB $CD34^+$ cells (2×10^4 or 1×10^5) or $CD34^-CD14^{+/-}$ cells (1×10^7) were injected through the tail vein. Neomycin sulfate (Invitrogen, Carlsbad, CA, USA) in acidic water was supplied to irradiated recipient mice after transplantation.

Flow cytometric analysis of peripheral blood from mice transplanted with human cells

The peripheral blood of mice was collected and transferred to ethylenediaminetetraacetic acid (EDTA) -2Na-containing CAPIJECT (Terumo Medical, Somerset, NJ, USA). The cells were then analyzed by flow cytometry (FACS caliber; BD PharMingen, San Diego, CA, USA) to measure the frequencies of various human hematopoietic cell types using the following antibodies (all purchased from BD PharMingen): fluorescein isothiocyanate- (FITC) and phycoerythrin- (PE) conjugated mouse anti-human CD3, CD4, CD8, CD14, CD19, CD33, CD45, and CD56, and allophycocyanin (APC)-conjugated rat anti-mouse CD45.

Detection of human CB-derived cells in the murine liver by immunohistochemical analysis

Mice were anesthetized, killed by cervical dislocation, and their livers were collected, fixed in 10% formalin, and embedded in paraffin blocks. Four-micrometer sections were cut and placed on silane-coated slides. After removing the paraffin with xylene, the tissue sections were rehydrated with graded alcohol, washed with water, and incubated with primary antibodies diluted with phosphate-buffered saline (PBS) or PBS containing 1% bovine serum albumin. The antibodies (and dilutions) used were rabbit anti-human albumin (1:100) (DAKO Carpinteria, CA, USA), mouse anti-human-specific hepatocyte antigen (HepPar1) (1:100) (DAKO), rabbit anti-human α-1-antitrypsin (1:100) (Neomarkers, Fremont, CA, USA), mouse anti-human CD45 (1:100) (DAKO), mouse

anti-human CD68 (1:100) (DAKO), mouse anti-human mitochondria (1:100) (Chemicon International, Inc., Temecula, CA, USA), and rabbit anti-human c-met (1:100) (Santa Cruz Biotechnology, Inc., Santa Cruz, CA, USA). All antibodies except for rabbit anti-human c-met were confirmed to be specific for the relevant human antigen by immunohistochemical assays using mouse control specimens (including those from irradiated mice). Three hours incubation at room temperature or an overnight incubation at 4°C was followed by incubation with the 1:100-diluted secondary antibodies: Cy3-conjugated donkey anti-mouse IgG, FITC-conjugated donkey anti-rabbit IgG, peroxidase-conjugated donkey anti-mouse, and peroxidase-conjugated donkey anti-rabbit IgG (all purchased from Jackson ImmunoResearch Laboratories, West Grove, PA, USA). Hoechst 33324 (Molecular Probes, Eugene, OR, USA) was used for nuclear staining. Endogenous peroxidase activity was blocked by application of 3% hydrogen peroxide for 5 min at room temperature and a DAB Substrate Kit (Vector Laboratories, Burlingame, CA, USA) was used for visualization. Antigen retrieval was performed by heating the sections in 10 mM citrate or 10 mM citrate/2 mM EDTA buffer in an autoclave oven for 5 min. These prepared samples were then examined under a light or fluorescent microscope (Olympus, Tokyo, Japan).

Serum human albumin enzyme-linked immunosorbent assay (ELISA)

Peripheral blood was collected into serum separator tubes (BD PharMingen) at various points after transplantation for the human serum albumin assays, and ELISA was performed according to the manufacturer's instructions (Cygnus Technologies, Plainville, MA, USA).

Flow cytometric analysis of single liver cells obtained by collagenase perfusion

Mice were anesthetized, their abdomens were opened, and their inferior vena cava was cannulated. The hepatic vein and whole liver were then retrogradely perfused gently at 37°C with Hanks' buffered salt solution (HBSS; Gibco BRL, Grand Island, NY, USA) containing 2-[4-(2-hydroxyethyl)-1-piperazinyl]ethanesulfonic acid (HEPES) at a final concentration of 10 mM (Nakalai Tesque, Inc., Kyoto, Japan) and ethyleneglycoltetraacetic acid at a final concentration of 0.5 mmol/l. This was followed by perfusion with HBSS containing HEPES (final concentration of 10 mM) and collagenase D (final concentration of 200 μg/ml) (Roche Diagnostics GmbH, Mannheim, Germany). After perfusion, a homogeneous liver cell suspension that contained hepatocytes, blood cells, and nonparenchymal cells was obtained by gentle mechanical dispersion and filtering through a 70 μm nylon mesh cell strainer. After centrifugation and resuspension in PBS with 2% fetal calf serum, this preparation was characterized by flow cytometric analysis using a Cytofix/CytoPerm kit (BD PharMingen). Briefly, the cells were stained with one of the following primary antibodies: APC-conjugated mouse anti-human CD45 (BD PharMingen); FITC-, PE-, or APC-conjugated mouse anti-human HLA-ABC (BD PharMingen); or PE-conjugated rat anti-mouse H-2K^{d} (BD PharMingen). The cells were then washed, fixed, and permeabilized with Cytofix/Cytoperm solution for 20 min. After washing with Perm/Wash buffer twice, cells were incubated with isotype IgG or rabbit anti-human albumin for 30 min at 4°C, followed by incubation with FITC-conjugated donkey anti-rabbit IgG for 30 min at 4°C. After washing with Perm/Wash, the cells were analyzed by flow cytometry.

Fluorescence *in situ* hybridization (FISH)

Cy3-dUTP-labeled human genome DNA probe and Cy5-dUTP-labeled mouse genome DNA probe were used simultaneously. Slides were heated to 45°C for 30 min, then deparaffinized and dried. Slides were then denatured for 5 min in 2× saline sodium citrate (SSC) buffer, microwaved for 10 min, digested with 0.1% pepsin/0.1M HCl for 5 min, and washed with PBS. After dehydration, probes were applied and sections were incubated at 90°C for 13 min for denaturation. After overnight incubation at 37°C, the sections were stringently washed in 2 × and 1× SSC containing 50% formamide. The nuclei were counterstained with 4',6-diamino-2-phenylindole and multicolored immunofluorescent staining was analyzed by a fluorescence microscope (Leica, Wetzlar, Germany).

Reverse transcription-polymerase chain reaction (RT-PCR)

Mice were anesthetized, then killed by cervical dislocation. Total RNA was extracted from chimeric liver, nontransplanted liver, irradiated liver, human liver, and human CB CD34^{+} cells using Trizol reagent (Invitrogen Corp., San Diego, CA, USA) according to the manufacturer's instructions. Equal amounts of RNA from all samples were subjected to first-strand cDNA synthesis with an oligo dT primer and Superscript II RT (Invitrogen Corp.) The cDNAs were then amplified using an AmpliTaqGold Kit (Applied Biosystems, Foster City, CA, USA) and human-specific primers. Amplification was performed at 95°C for 5–10 min, followed by 30–40 cycles of 94–95°C for 30 s, 56–60°C for 30–60 s, and 72°C for 60 s, with a final extension at 72°C for 7 min. The primers and PCR reaction conditions used are detailed in **Table 1**. The PCR products were separated by electrophoresis in 1% agarose gels, stained with ethidium bromide, and photographed.

Real-time quantitative RT-PCR analysis

Forward and reverse primers as well as fluorogenic probes were designed according to Perkin-Elmer guidelines (Primer Express Software). Human glyceraldehyde 3-phosphate dehydrogenase (GAPDH) primers and probes were purchased from Applied Biosystems. Quantitative assessment of mRNA expression was performed using a human GAPDH internal standard. The expression of each mRNA was compared with each human liver mRNA expression. The primers and probes are detailed in **Table 2**.

Statistical analysis

Statistical significance was determined by using the Pearson's correlation coefficient test.

RESULTS

Large numbers of human liver parenchymal and nonparenchymal cells are present in the murine liver after human CB CD34^{+} cell transplantation

We transplanted liver-intact NOD/SCID/γ_c^{null} mice with purified human CB CD34^{+} cells and subjected the livers to immunohistochemical analysis at various time points to determine whether the murine livers contain hepatic cells derived from human CB CD34^{+} cells.

TABLE 1. *The primers and PCR reaction conditions*

Genes	Primers		Annealing (°C)	Cycles
	Sense (5' to 3')	Antisense (5' to 3')		
Albumin #1	gaacttcgggatgaagggaa	gcaagtcagcaggcatctca	59	40
Albumin #2	aacgccaagtaagtgacaga	gaaaagaaaaacagatgaa	56	40
Alpha1AT	ctttgaagtcaaggacaccg	gctgaagaccttagtgatgc	56	35
Transferrin	cctgatccatgggctaagaa	ctacggaaagtgcaggcttc	58	35
RBP4	gcctctttctgcaggacaac	cgggaaaacacgaaggagta	60	40
Prealbumin	cagaaaggctgctgatgaca	caggtccactggaggagaag	59	40
CPSI	gttgtctgaaccaagcagca	cgcagtgtgcggatactaga	60	40
CYP3A4	tgtgaggaggtagatttggctc	tcaggaggagttaatggtgctaa	59	40
TAT	cgcagattactcccttgctc	gtgtccccaacttctttcca	58	40
TO	tgcagcagttttccattctg	tcagccacctgttcctcttt	56	40
FVIII	tgccacaactcagactttcg	gtcgcaagagcatcaacaaa	56	40
CK7	caggaactcatgagcgtgaa	gggtgggaatcttcttgtga	58	40
CK19	aggtggattccgctccgggca	atcttcctgtccctcgagca	58	40
eNOS	tgctggcatacaggactcag	taggtcttggggttgtcagg	59	40
Human HPRT	aattatggacaggactgaacgtc	cgtggggtccttttcaccagcaag	60	35
Mouse HPRT	gctggtgaaaaggacctct	cacaggactagaacacctgc	59	30

TABLE 2. *Primers and probes for real-time quantitative RT-PCR*

Genes	Primers		Probes
	Sense (5' to 3')	Antisense (5' to 3')	
Albumin	ttaccaaagtccacacggaatg	caaggtccgccctgtcat	tgccatggagatctgcttgaatgtgct
CK7	gcgtgagtaccaggaactcatg	gcttgcggtaggtggcg	tgaagctggccctggacatcgaga
CPSI	ggcaatgctttccacagga	ttggccggaatgattgct	agataccccagaaaggcatcctgataggcat
TAT	gactcgggcaaatataatggct	gcaatctcctcccgactgg	tgccccatccatcggcttcc

TABLE 3. *Correlation between frequency of human albumin-positive cells by immunohistochemistry and the levels of human albumin in the blood of recipient mice*

Mouse	Time after transplantation	Frequency of human albumin-positive cells by immunohistochemistry (%)	Serum human albumin (μg/ml)
#1	3 months	1.67(17/1019)	0.8
#2	3 months	2.15(22/1023)	0.6
#3	5 months	2.56(28/1094)	1.4
#4	5 months	2.61(33/1263)	2.3
#5	6 months	3.43(32/933)	3.7

Human albumin-expressing cells were invariably found in the livers of all the recipient mice. Some formed large clusters around the portal veins (**Fig. 1*A***) whereas others were scattered throughout the liver lobule and showed a punctuate distribution away from the portal veins (Fig. 1*B*). Double staining for human albumin and human-specific hepatocyte antigen (HepPar1) revealed that the human albumin-positive cells were also HepPar1-positive (Fig. 1*C, D*).

Because the liver contains a large amount of peripheral blood, we checked the distribution of human peripheral blood cells. Double staining of the liver sections for human CD45 and human albumin revealed small, round, human CD45-positive peripheral blood cells beneath the basal membrane of the portal veins and in the sinusoidal area of the livers (Fig. 1*E, F*); an anti-human albumin antibody stained a different population of cells in the same section. We also detected human α-1-antitrypsin-positive cells in the liver (Fig. 1*H*), which indicates the functional maturation of human CB-derived hepatocytes; these cells were also present in a section of human liver used as a positive control (Fig. 1*G*). These hepatocytes were first detected 1 month after transplantation and tended to increase in number with time (data not shown).

Kupffer cells are spindle-shaped; they are located between hepatocytes and retain macrophage markers such as CD68 (27) (**Fig. 2*A***). Mature human Kupffer cells were present in the murine liver environment of the recipient mice (Fig. 2*B*). Murine Kupffer cells were not stained by anti-human CD68 antibody (Fig. 2*C*).

We assessed the ability of human CB $CD34^+$ cells to

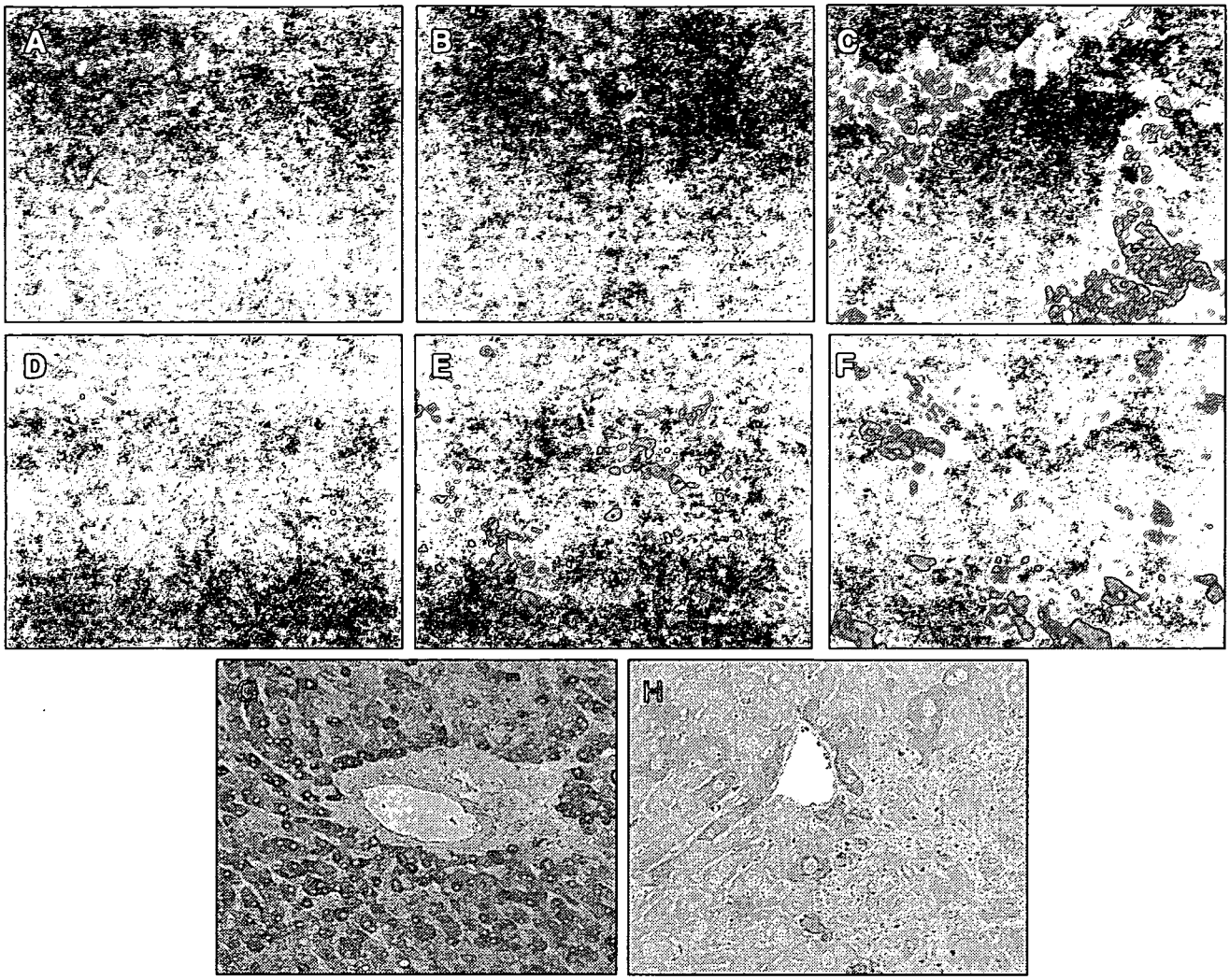

Figure 1. Large numbers of human CB CD34$^+$ cell-derived liver parenchymal cells are found in the livers of recipient mice. *A, B)* Human albumin-expressing cells in murine liver sections were identified using an FITC-labeled anti-human albumin antibody. *C, D)* Triple staining of murine liver sections for human albumin (green), human HepPar1 (red) and nuclei (blue). *E, F)* Triple staining of murine liver sections for human albumin (green), human CD45 (red), and nuclei (blue). *G)* Immunohistochemical analysis of a human liver section as a positive control for human α-1-antitrypsin staining. *H)* Identification of human α-1-antitrypsin-expressing cells in transplanted murine liver sections.

produce cholangiocytes by immunohistochemistry with antibodies for human mitochondria and c-met. The antibody for c-met is reported to recognize both hepatocytes and cholangiocytes, particularly when they are proliferating (28, 29). Cube-shaped cholangiocytic cells in the recipient livers were positive for human mitochondria and c-met, which suggests that these cells are of human origin (Fig. 2*D–F*). Indeed, we identified 250 portal areas from 10 independent mice and found three ducts containing human marker (human mitochondria).

To exclude the possibility that 240cGy radiation might induce liver injury, we evaluated the liver after radiation. Histology showed no liver damages such as inflammation, lobar necrosis, or fibrosis. We could not detect TUNEL (TdT-mediated dUTP-biotin nick end labeling)-positive cells. Furthermore, serum AST/ALT levels did not increase (data not shown).

These results indicate that human CD34$^+$ cells can produce human hepatocytes, Kupffer cells, and cholangiocytes in the murine liver environment; these cells develop even in the absence of massive hepatotoxic damage.

Human albumin is present in the peripheral blood of recipient mice and increases with time after transplantation

To check whether the human albumin-positive cells in the livers of recipient mice have the ability to secrete albumin into the murine bloodstream, we measured levels of human albumin in the blood of recipient mice by ELISA at various points after the transplantation. We could not detect human albumin at all in the peripheral blood of either untransplanted mice (n=5) or mice within 2 months after transplantation (n=5) (**Fig. 3*A***

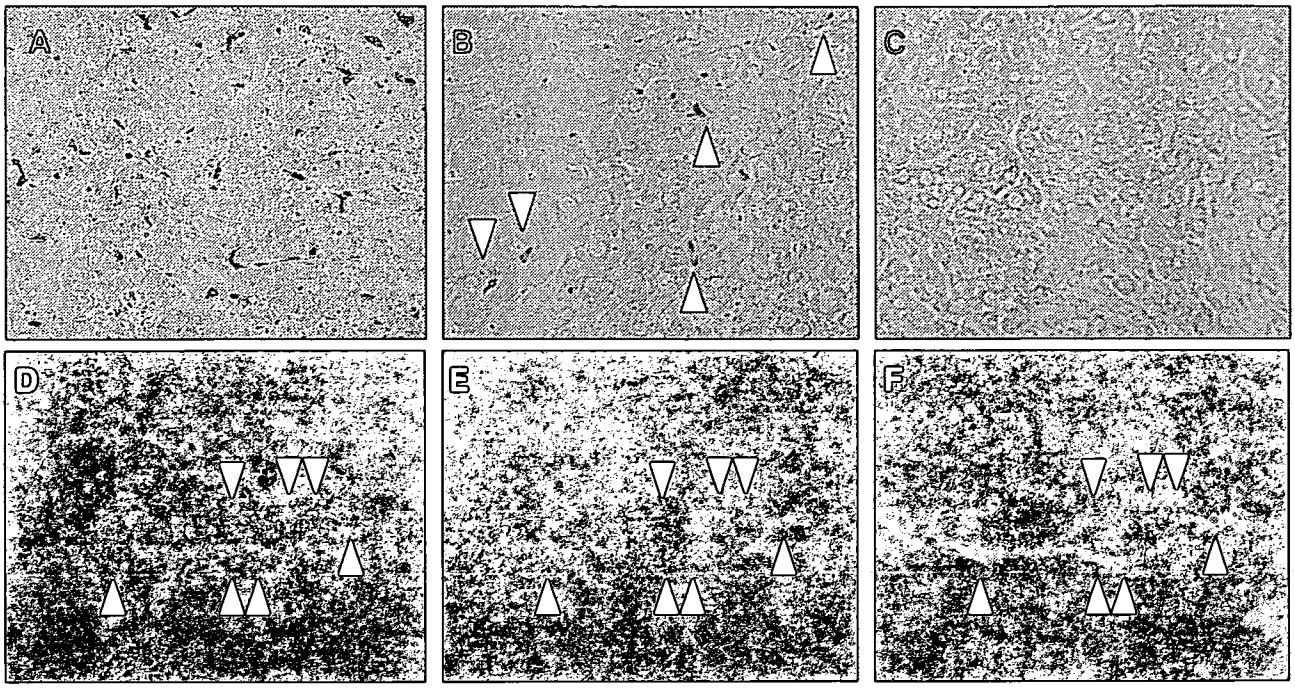

Figure 2. Kupffer cells and cholangiocytes derived from human CB $CD34^+$ cells are present in the transplanted murine liver. *A)* Immunohistochemical analysis of a human liver section as a positive control for human CD68 staining. *B)* Liver sections of a recipient mouse. Human CD68-expressing cells were identified by staining with an HRP-labeled anti-human CD68 antibody. *C)* Murine Kupffer cells were not stained by anti-human CD68 antibody. *D, F)* Liver sections from recipient mice were analyzed for the presence of human mitochondria-positive cells (stained red, *D)* and human or mouse c-met-positive cells (green, *E*). The two images in panels *D, E* are merged in panel *F*. Arrowheads indicate the human mitochondria-positive cells. Nuclei are stained blue.

and data not shown). Serum human albumin was first detected 3 months after transplantation, and the levels increased gradually with time after transplantation. In addition, the human albumin levels increased in all four mice whose levels we measured serially (Fig. 3*A*). These results indicate that human CB $CD34^+$ cells can generate human albumin-positive cells continuously in the murine liver and that these cells become mature enough to secrete albumin from their cytoplasm into the bloodstream. Indeed, we found a positive correlation between the frequency of human albumin-positive cells determined by immunohistochemistry and levels of human albumin in the blood of recipient mice (Table 3).

Human albumin levels in the peripheral blood of recipient mice correlate with the degree of peripheral blood chimerism and human T cell frequencies

Using flow cytometry, we detected various types of human hematopoietic cells in the peripheral blood of the recipient mice, including T cells ($CD3^+$, $CD4^+$, $CD8^+$), B cells ($CD19^+$), myelomonocytic cells ($CD14^+$, $CD33^+$), and NK cells ($CD56^+$) (Fig. 3*B* and data not shown). This is consistent with previously reports (24, 25). We examined whether the human CB $CD34^+$ cells first give rise to a particular hematopoietic cell population in the peripheral blood and then participate in producing the human cell-derived hepatocytes in the recipient mice. To address this question, we first asked whether the chimerism of the liver in the recipient mice (defined as the levels of human albumin in the serum) correlated with the chimerism of the whole peripheral blood cell population (defined as the percentage of human $CD45^+$ cells relative to all mouse and human $CD45^+$ cells). We found a strong positive correlation between the chimerism of the liver and the whole peripheral blood cell population (Fig. 3*C*). We then examined whether the liver chimerism correlated with the percentages of particular types of human leukocytes in the peripheral blood. We found that the percentage of human T cells (human $CD3^+$ cells) most strongly correlated with the levels of human albumin in the serum (Fig. 3*D*). The percentage of human myelomonocytic cells [defined as either human $CD45^+$ minus ($CD3^+$ plus $CD19^+$) or human $CD14^+$] correlated weakly with the human albumin levels (Fig. 3*D* and data not shown). In contrast, the human albumin levels did not correlate with human B cell (human $CD19^+$) frequency (Fig. 3*D*).

Human albumin-positive cells in the livers of recipient mice express both human and mouse markers, suggesting that cell fusion occurs

We next characterized the human hepatocytes and blood cells in the recipient mice by assessing their expression of various surface markers and intracellular

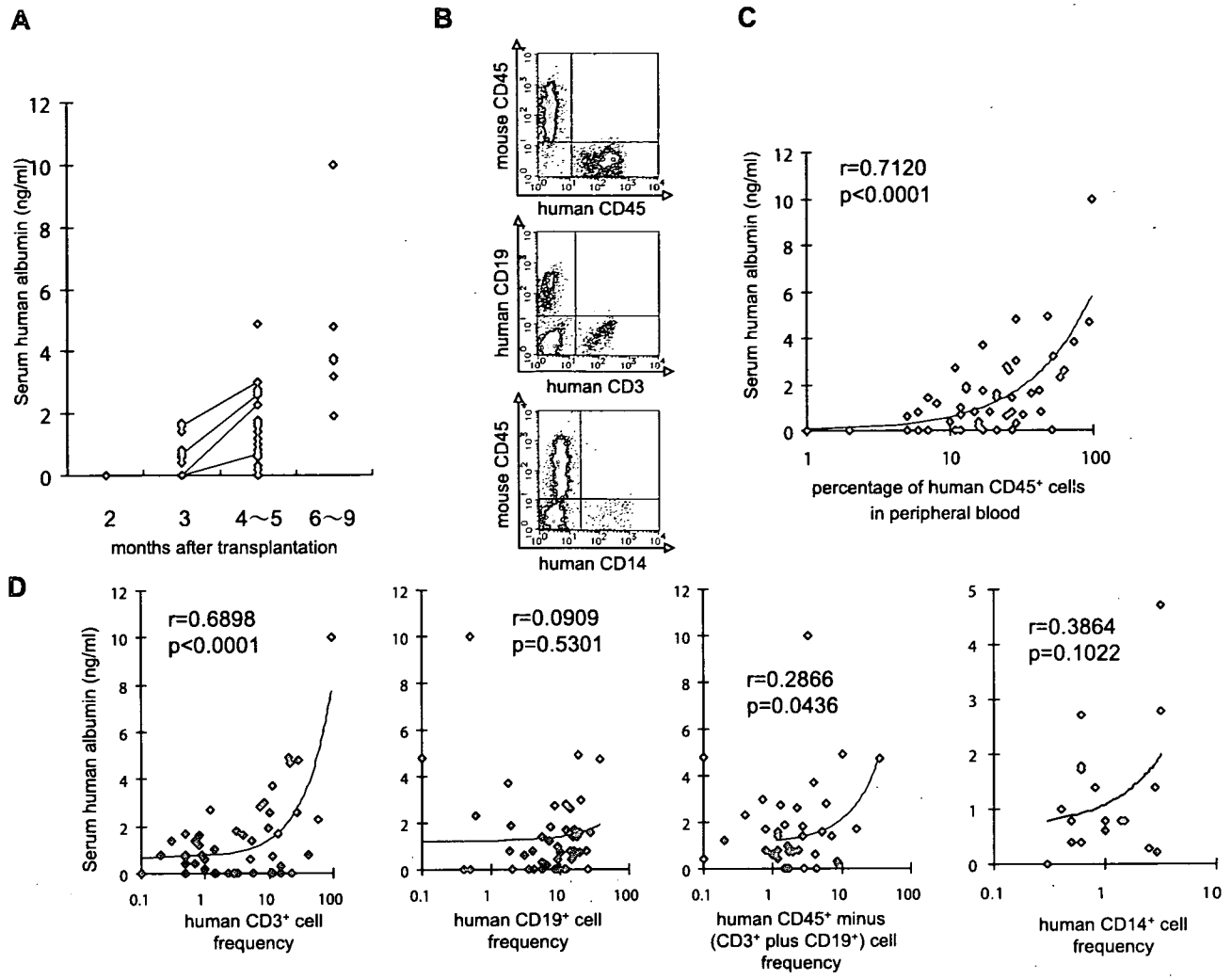

Figure 3. Levels of human albumin in the blood of recipient mice correlate with time after transplantation, the degree of overall peripheral blood chimerism, and human $CD3^+$ T cell frequencies. *A)* Serum human albumin was detected by ELISA for the first time 3 months after transplantation. Human albumin levels in the peripheral blood of recipient mice increased gradually with time after transplantation. The bars connecting the symbols indicate serial measurements in the same mice. *B)* The peripheral blood of the recipient mice contained a variety of human cells. *C)* Relationship between the human albumin levels in the peripheral blood and the chimerism of the peripheral blood. The regression line is indicated. *D)* The relationship between the human albumin levels in the peripheral blood and the percentage of human $CD3^+$ T cells, human $CD19^+$ B cells, and myelomonocytic cells (human $CD45^+$ minus [$CD3^+$ plus $CD19^+$] cells or $CD14^+$ cells).

proteins by flow cytometry. We first obtained cells from the liver by two-step collagenase perfusion at least 3 months after the transplantation (**Fig. 4*A***). When the dissociated cells from untransplanted control mice were plotted on the basis of their forward scatter and side scatter, we identified two regions: R1 and R2 (Fig. 4*B*). R1 contained mature hepatocytes whereas R2 contained $CD45^+$ hematopoietic cells (data not shown). For the recipient mice, 0.88% to 4.73% of the cells in R1 (mean 2.73%) were positive for human albumin (see R4 in Fig. 4*C, D*). These human albumin-positive cells were distinguishable from the human $CD45^+$ hematopoietic cells (see R5 in Fig. 4*C*). We confirmed that the human albumin-positive cells and human $CD45^+$ cells expressed human HLA-ABC (Fig. 4*E*). Staining with an anti-mouse $H\text{-}2K^d$ antibody revealed that the human albumin-positive cells also expressed the murine MHC class I molecule (Fig. 4*F*). In contrast, human $CD45^+$ cells in the liver were negative for mouse $H\text{-}2K^d$ (Fig. 4*G*). These data suggest that the human albumin-positive hepatocytes in this model were produced by cell fusion.

The livers of recipient mice contain nucleus positive for both human and mouse genomic DNAs

To clarify the genetic content of the human albumin-positive hepatocytes, we performed FISH for human

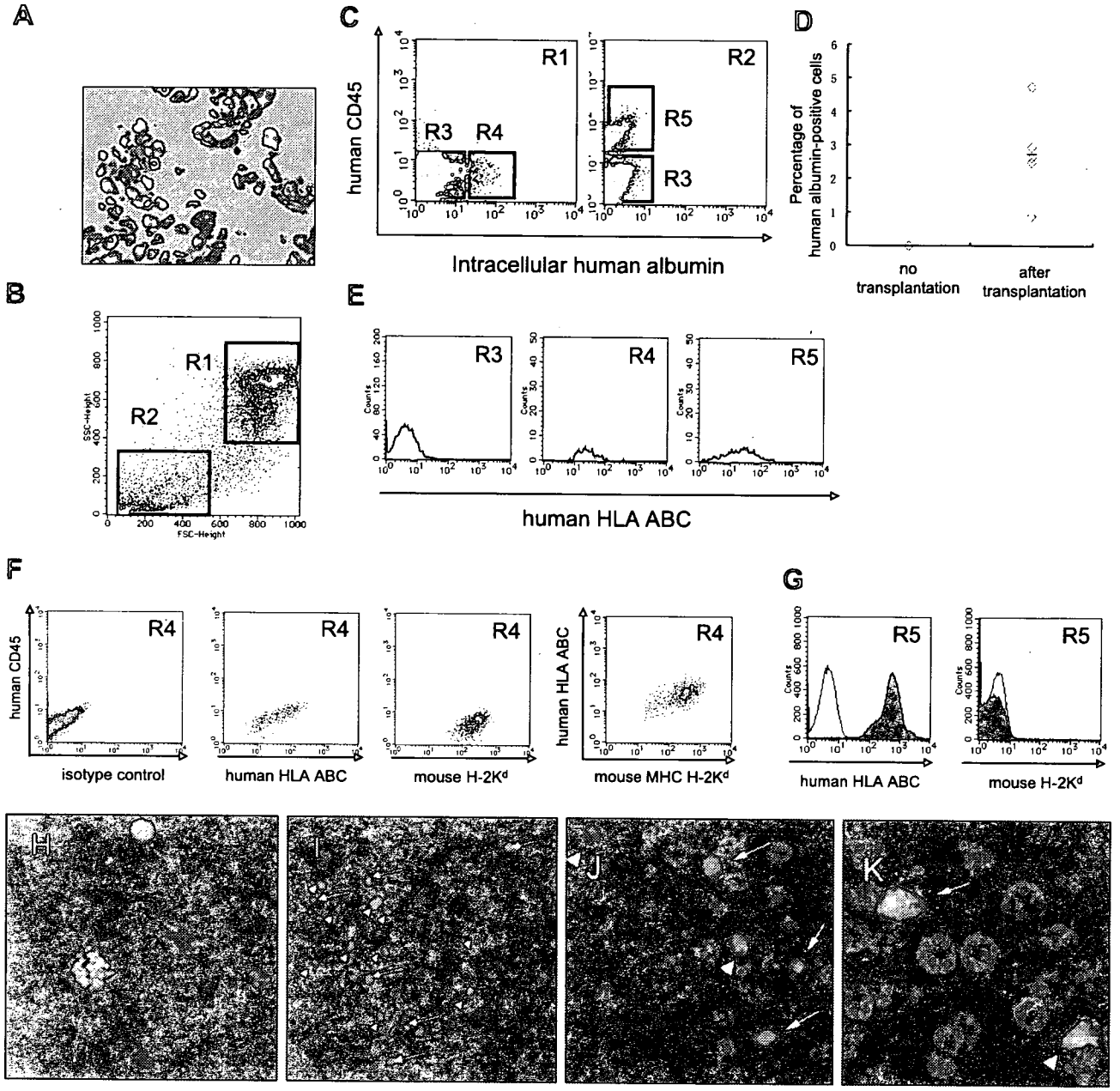

Figure 4. Human CB-derived albumin-positive hepatocytes possess both human and mouse markers, suggesting that cell fusion occurs. *A)* The murine liver after collagenase perfusion. Single cells of various sizes and shapes were acquired. *B)* Flow cytometric analysis of the dissociated liver cells. These cells were divided into two types on the basis of their size and granularity, as shown by regions R1 and R2. *C)* Staining of the dissociated liver cells from recipient mice with anti-human CD45 and anti-human albumin antibodies resulted in three regions: double-negative cells (R3), human albumin-positive cells (R4), and human CD45$^+$ cells (R5). Note that the human albumin-positive cells belong to R1 whereas the human CD45$^+$ cells belong to R2. *D)* The percentage of liver cells from recipient mice that were human albumin-positive in R1 ranged from 0.88% to 4.73%. *E)* Analysis of human HLA-ABC expression by the cells in R3, R4, and R5. The cells in both R4 and R5 express human HLA-ABC whereas the cells in R3 do not. *F)* Analysis of human HLA-ABC and mouse H-2K^d expression by human albumin-positive cells. Note that these cells expressed both human and murine MHC class I molecules. *G)* Analysis of human HLA-ABC and mouse H-2K^d expression by human CD45-positive cells. These cells expressed the human MHC class I molecule but not the murine MHC class I molecule. *H)* Verification of human (yellow) and mouse (red)-specific genomic DNA probe. *I–K)* Triple staining of murine liver sections for human DNA (yellow), mouse DNA (red), and nuclei (blue). Arrows indicate the presence of fusion-derived nuclei. The nuclei of human peripheral blood cells were also identified (arrowheads).

and mouse genomic DNA. Figure 4*H* illustrates the verification of probes on a test specimen. Figure 4*I–K* demonstrates detection of human and mouse genomic DNA on the livers of recipient mice, revealing the presence of a single nucleus positive for both human and mouse genome. The percentage of these nuclei ranged from 2 to 5%, similar to the frequency of human albumin-positive cells determined by immuno-

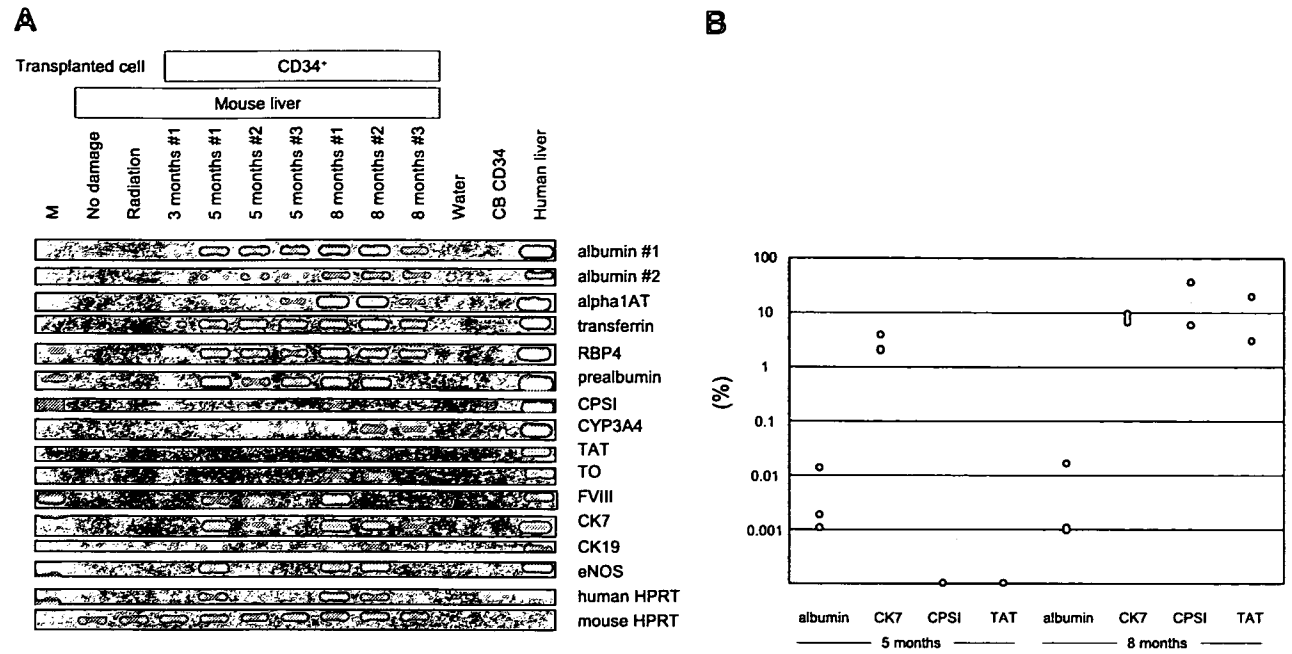

Figure 5. Up-regulation of a wide variety of human liver-specific mRNAs in the livers of human CB $CD34^+$-recipient mice. *A)* M, size marker; radiation, 240cGy radiation; α1 AT, α-1-antitrypsin; RBP4, retinol binding protein 4; CPSI, carbamoyl phosphate synthetase I; TAT, tyrosine aminotransferase; TO, tryptophan-2,3-dioxygenase; FVIII, coagulation factor VIII; CK7, cytokeratin 7; CK19, cytokeratin 19; eNOS, endothelial nitric oxide synthase; HPRT, hypoxanthine guanine phosphoribosyl transferase. Chimeric samples were collected at the indicated time points after transplantation. *B)* Real-time quantitative RT-PCR analysis. The comparative cycle threshold (C_T) method was used to determine the relative expression levels of human albumin, CK7, CPSI, and TAT. The threshold cycles for each gene and human GAPDH were determined and the cycle number difference (ΔC_T) was calculated for each replicate. Relative expression values were calculated using the mean of ΔC_T from the 3 replicates and expressed as $2^{(\Delta C_T)}$.

histochemistry. These data showed that nuclear fusion occurred in the livers of recipient mice.

A wide variety of human liver-specific mRNAs are transcribed in the CB-derived human hepatocytes in the murine liver

We next used RT-PCR to analyze the murine liver for the presence of human albumin mRNAs after human CB $CD34^+$ cell transplantation into liver-intact mice (**Fig. 5*A***). We first used two different primer pairs to assess the presence of human albumin mRNA, which we detected in the livers of all seven mice transplanted with human CB $CD34^+$ cells. We confirmed that neither the livers of untransplanted mice nor human CB $CD34^+$ cells expressed human albumin mRNA. Human albumin mRNAs were expressed just 1 month after transplantation (data not shown).

We then examined the samples for mRNA expression of other human hepatic parenchymal and nonparenchymal markers. To our surprise, we found that a wide variety of human liver-specific mRNAs were newly transcribed: human α-1-antitrypsin (α1AT), transferrin and retinol binding protein 4 (RBP4) and prealbumin (all of which are rapid turnover proteins), carbamoyl phosphate synthetase I (CPSI), CYP3A4, tyrosine aminotransferase (TAT) and tryptophan-2,3-dioxygenase (TO) (all of which serve as terminal hepatic differentiation markers), coagulation factor VIII (FVIII), cytokeratin 7 (CK7), cytokeratin 19 (CK19), and endothelial nitric oxide synthase (eNOS). All of these genes were expressed in the livers of the recipient mice in the absence of any liver damage. We also found that human CK18 mRNA (mature hepatocyte marker; ref. 21) was newly transcribed in the livers of all seven mice transplanted, although we found that CB CD34+ cells also expressed it (data not shown). It is notable that, as with albumin, the percentage of mice with livers bearing human liver-specific mRNA tended to rise with time after transplantation. Furthermore, using real-time quantitative RT-PCR analysis, we confirmed expression levels of the human albumin, CK7, CPS1, and TAT in chimeric livers (Fig. 5*B*). The levels of these genes also tended to rise higher with time after transplantation, and some exceeded 10% compared with those of human livers. These data indicate that human CB $CD34^+$ cells, which are initially destined to become mature blood cells, begin human liver-specific gene transcription in the murine liver through cell fusion.

Human CB $CD34^+$ cells can develop into human albumin-positive hepatocytes whereas $CD34^-$ cells cannot

To test whether $CD34^-$ cells can develop into mature hepatocytes in the murine liver as $CD34^+$ cells do, we

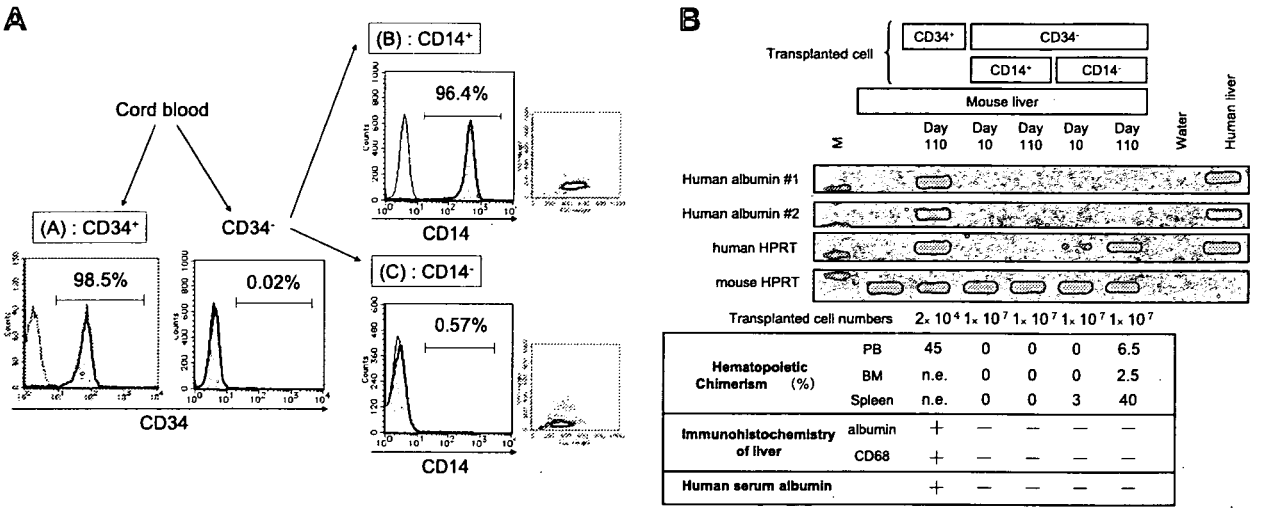

Figure 6. Comparison of the hepatocyte-producing ability of human CB $CD34^+$ and $CD34^-$ cells. *A)* Depiction of the process used to prepare the transplantable cell populations and analysis of their purity by flow cytometry. *B)* $CD34^+$ cells generated high numbers of human blood cells and human albumin-positive cells (as shown by immunohistochemistry) as well as considerable amounts of human albumin mRNA levels in the liver (as shown by RT-PCR) and human albumin protein levels in the murine bloodstream, whereas $CD34^-$ cells did not. Each column in the table refers to the lane directly above it. M, size marker; n.e., not examined.

sorted the CB from the same donor into three populations and injected each i.v. into NOD/SCID/γ_c^{null} mice: *1)* $CD34^+$ cells, *2)* $CD34^-CD14^+$ cells (monocytes), and *3)* $CD34^-CD14^-$ cells (T cells, B cells, NK cells, mesenchymal stem cells (MSCs), and others). A flow cytometric analysis showed that contamination of the $CD34^-$ groups with $CD34^+$ cells was negligible and that the $CD14^+$ and $CD14^-$ cells were efficiently separated by cell sorting (**Fig. 6A**). Although 2×10^4 $CD34^+$ cells generated large numbers of functional hematopoietic and hepatic cells that expressed human markers, no human albumin expression was detected in the liver at either day 10 or day 110 when 1×10^7 $CD34^-14^+$ or $CD34^-14^-$ cells were transplanted (500-fold the $CD34^+$ cell dose) (Fig. 6*B*). In the case of $CD34^-14^-$ cells transplantation, significant hematopoietic chimerism came from temporarily expanding donor T cells. Indeed, all the hematopoietic cells in these mice are CD3 positive. These results clearly show that only human CB $CD34^+$ cells, and not $CD34^-$ cells, can generate human albumin-expressing cells in the livers of recipient mice in our model.

DISCUSSION

Lagasse *et al.* (2) were the first to demonstrate that purified hematopoietic stem cells can differentiate into hepatocytes *in vivo*. Subsequently, congenic mouse-to-mouse transplantation of bone marrow populations rich in hematopoietic stem cells was used to show hepatic differentiation of hematopoietic cells. However, it is controversial how hematopoietic stem cells generate hepatocytes. Many researchers have used the human-to-mouse xenogeneic transplantation model, but with extremely low efficiency (<0.5%), making it difficult to analyze the mechanism by which hematopoietic stem cell transplantation induces liver regeneration. We previously demonstrated that NOD/SCID/γ_c^{null} mice show superior efficient human hematopoietic stem cell engraftment (24, 25). In the current study, small numbers of $CD34^+$ cells (which represent hematopoietic stem cells) were transplanted to exclude the effects of other cells types (*e.g.*, the $CD34^-$ MSCs and other unknown stem cells). We demonstrated that the livers of the recipient mice expressed human albumin, HepPar1, and α-1-antitrypsin protein. In addition, we detected considerable numbers of human albumin-positive cells (an average of 2.73% of the total number of hepatocytes) by flow cytometry. These numbers are close to the numbers detected in the clinical human-to-human transplantation cases. We also detected human albumin in the murine bloodstream. Finally, we revealed that livers of the recipient mice express a variety of human liver-specific genes. These findings suggest that functional human hepatic cells develop in the liver after transplantation of human CB $CD34^+$ cells into liver-intact NOD/SCID/γ_c^{null} mice.

Results showing that *1)* the human albumin-positive hepatocytes expressed not only human HLA-ABC, but also mouse H-$2K^d$, and that *2)* the livers of recipient mice contained nucleus positive for both human and mouse genomic DNAs strongly support not transdifferentiation, but cell fusion, as the main mechanism of this phenomenon. This appears to contrast with the conclusions drawn from some other human-to-mouse models (16, 19). It is possible that, in our model, the human hematopoietic cells are abundantly supplied from bone marrow to the systemic circulation, and that

they infiltrate the liver and have more opportunity to develop into functional human hepatic cells through cell fusion due to the far better human hematopoietic stem cell engraftment.

We found that human albumin levels in the peripheral blood correlated strongly with the overall peripheral blood chimerism and the numbers of human T cells in the peripheral blood, but correlated weakly with the numbers of human myelomonocytic cells in the peripheral blood. However, our short-term and long-term observations revealed that neither $CD34^-CD14^+$ cells (monocytes) nor $CD34^-CD14^-$ cells (T cells, B cells, NK cells, MSCs, and others) could produce albumin-positive cells. This shows that although these terminally differentiated human cells (T cells and myelomonocytic cells) or MSCs may contribute to human liver regeneration indirectly, each alone might be insufficient to become a direct fusion partner. Previous studies have shown that myelomonocytic cells are sufficient for generating hepatocytes in mouse cells (10, 11). Selzner *et al.* (30) also proposed that Kupffer cells, which reside in the sinusoids and produce cytokines, recruit other cells or release TNF-α and IL-6, which then initiate hepatocyte proliferation *in vivo*. Some of our findings support the possibility that myelomonocytic cells or Kupffer cells may to some extent drive the production of human albumin-positive hepatocytes: we detected a weak positive correlation between human myelomonocytic cells and human albumin levels, and detected human $CD68^+$ Kupffer cells in the transplanted murine livers. However, our data showed that *1)* human CB $CD34^-CD14^+$ cells alone did not develop into human albumin-positive cells, and *2)* many of the human albumin-positive cells we detected by immunohistochemistry were not located adjacent to $CD68^+$ Kupffer cells (data not shown). These observations may suggest that the production of human albumin-positive cells, at least in our model, cannot be explained merely by direct cell fusion between myelomonocytic cells/Kupffer cells and hepatocytes, as has been shown in mouse-to-mouse transplantation studies (10, 11). Nevertheless, our experiment cannot exclude the possibility that differentiated progeny of human hematopoietic stem cells fuse with hepatocytes, considering the very long lag time between transplantation of CD34+ cells and the increase in albumin levels. If we transplanted more cells or chose a different mode of transplantation, we could achieve a more efficient deposition of cells in the liver and could detect the fusion of infused human cells. Recently, Manz *et al.* (31) showed the prospective isolation of the human clonogenic common myeloid progenitors and their downstream progeny. The transplantation of highly purified hematopoietic intermediates helps us to better understand the ability to fuse them with hepatocytes.

A striking observation from our study is that CB $CD34^+$ cells are transcriptionally converted into liver cells after entering the liver of NOD/SCID/γ_c^{null} mice even in the absence of damage-associated stimuli other than a small dose of total body irradiation (with which the mice are preconditioned prior to transplantation). It is generally believed that tissue damage is indispensable for the hematopoietic-to-hepatic cell lineage transition (1) except for the FAH mouse model (32). However, we found that even without massive liver damage, human CB $CD34^+$ cells or their progeny cells could fuse with hepatocytes of NOD/SCID/γ_c^{null} mouse, lose their hematopoietic surface markers (CD45), and up-regulate human liver-specific gene transcription, contrary to other human-to-mouse xenogeneic transplantation models (17, 18, 20–23). There may be several reasons why a wide variety of human hepatocyte-specific genes are so efficiently transcribed and translated in our liver-intact NOD/SCID/γ_c^{null} mouse model. First, the NOD/SCID/γ_c^{null} mice may provide murine liver-specific transcription factors that promote human liver-specific gene transcription. It is possible that different strains of xenograft recipients may have different liver environments with respect to liver-specific transcription factors and that these differences influence the efficiency with which human cells with different properties are developed. Second, the observation that human albumin levels in the peripheral blood correlated strongly with human $CD3^+$ T cell levels suggests that these human T cells in murine liver may, not directly but indirectly, induce the hepatocyte development pathway *in vivo*. Further study is needed to clarify how the transcription of liver-specific genes is up-regulated in nuclei once cells are committed to a hematopoietic lineage. In our model, it took several months to up-regulate mature liver-specific genes. One explanation for the delay in hepatocyte gene activation is that in the case of donor-derived cells emerging around portal veins, cell fusion might have occurred with a progenitor cell, and thus maturation happened slowly.

We transplanted CB CD34+ cells into NOD/SCID/γ_c^{null} mice without irradiation but could not observe either hematopoietic engraftment or human hepatocytes in the liver of recipient mice. Therefore, we could not determine the influence of radiation on the frequency of cell fusion. With regard to the human albumin level in the peripheral blood of recipient mice, levels would be expected to be in micrograms per milliliter, not only nanograms per milliliter. Human albumin mRNA levels quantitated by real-time PCR were also low. There seem to be additional factors that control production and secretion of the albumin into the bloodstream of the mice. This awaits further investigation.

Using immunohistochemistry, we also showed that some cholangiocytes express human markers (human mitochondria). Whether this hematopoietic-to-cholangiocytic transition is due to transdifferentiation or cell fusion remains to be elucidated.

In conclusion, we have established a new model of efficient hematopoietic-to-nonhematopoietic transition. This experimental model system allows the formation of relatively large numbers of human-derived hepatic cells under near-physiological conditions, a

valuable tool for investigating the development of functional human hepatic cells from hematopoietic cells. Further elucidation of the molecular mechanisms by which blood cells efficiently become liver cells will greatly promote the feasibility of using conventional hematopoietic stem cell transplantation to treat patients with liver dysfunction. FJ

REFERENCES

1. Fausto, N. (2004) Liver regeneration and repair: hepatocytes, progenitor cells, and stem cells. *Hepatology* **39,** 1477–1487
2. Lagasse, E., Connors, H., Al-Dhalimy, M., Reitsma, M., Dohse, M., Osborne, L., Wang, X., Finegold, M., Weissman, I. L., and Grompe, M. (2000) Purified hematopoietic stem cells can differentiate into hepatocytes in vivo. *Nat. Med.* **6,** 1229–1234
3. Terada, N., Hamazaki, T., Oka, M., Hoki, M., Mastalerz, D. M., Nakano, Y., Meyer, E. M., Morel, L., Petersen, B. E., and Scott, E. W. (2002) Bone marrow cells adopt the phenotype of other cells by spontaneous cell fusion. *Nature* **416,** 542–545
4. Ying, Q. L., Nichols, J., Evans, E. P., and Smith, A. G. (2002) Changing potency by spontaneous fusion. *Nature* **416,** 545–548
5. Wang, X., Willenbring, H., Akkari, Y., Torimaru, Y., Foster, M., Al-Dhalimy, M., Lagasse, E., Finegold, M., Olson, S., and Grompe, M. (2003) Cell fusion is the principal source of bone-marrow-derived hepatocytes. *Nature* **422,** 897–901
6. Vassilopoulos, G., Wang, P. R., and Russell, D. W. (2003) Transplanted bone marrow regenerates liver by cell fusion. *Nature* **422,** 901–904
7. Alvarez-Dolado, M., Pardal, R., Garcia-Verdugo, J. M., Fike, J. R., Lee, H. O., Pfeffer, K., Lois, C., Morrison, S. J., and Alvarez-Buylla, A. (2003) Fusion of bone-marrow-derived cells with Purkinje neurons, cardiomyocytes and hepatocytes. *Nature* **425,** 968–973
8. Jang, Y. Y., Collector, M. I., Baylin, S. B., Diehl, A. M., and Sharkis, S. J. (2004) Hematopoietic stem cells convert into liver cells within days without fusion. *Nat. Cell Biol.* **6,** 532–539
9. Harris, R. G., Herzog, E. L., Bruscia, E. M., Grove, J. E., Van Arnam, J. S., and Krause, D. S. (2004) Lack of a fusion requirement for development of bone marrow-derived epithelia. *Science* **305,** 90–93
10. Willenbring, H., Bailey, A. S., Foster, M., Akkari, Y., Dorrell, C., Olson, S., Finegold, M., Fleming, W. H., and Grompe, M. (2004) Myelomonocytic cells are sufficient for therapeutic cell fusion in liver. *Nat. Med.* **10,** 744–748
11. Camargo, F. D., Finegold, M., and Goodell, M. A. (2004) Hematopoietic myelomonocytic cells are the major source of hepatocyte fusion partners. *J. Clin. Invest.* **113,** 1266–1270
12. Alison, M. R., Poulsom, R., Jeffery, R., Dhillon, A. P., Quaglia, A., Jacob, J., Novelli, M., Prentice, G., Williamson, J., and Wright, N. A. (2000) Hepatocytes from non-hepatic adult stem cells. *Nature* **406,** 257
13. Theise, N. D., Nimmakayalu, M., Gardner, R., Illei, P. B., Morgan, G., Teperman, L., Henegariu, O., and Krause, D. S. (2000) Liver from bone marrow in humans. *Hepatology* **32,** 11–16
14. Korbling, M., Katz, R. L., Khanna, A., Ruifrok, A. C., Rondon, G., Albitar, M., Champlin, R. E., and Estrov, Z. (2002) Hepatocytes and epithelial cells of donor origin in recipients of peripheral-blood stem cells. *N. Engl. J. Med.* **346,** 738–746
15. Ng, I. O., Chan, K. L., Shek, W. H., Lee, J. M., Fong, D. Y., Lo, C. M., and Fan, S. T. (2003) High frequency of chimerism in transplanted livers. *Hepatology* **38,** 989–998
16. Ishikawa, F., Drake, C. J., Yang, S., Fleming, P., Minamiguchi, H., Visconti, R. P., Crosby, C. V., Argraves, W. S., Harada, M., Key, L. L., Jr., Livingston, A. G., Wingard, J. R., and Ogawa, M. (2003) Transplanted human cord blood cells give rise to hepatocytes in engrafted mice. *Ann. N. Y. Acad. Sci.* **996,** 174–185
17. Kakinuma, S., Tanaka, Y., Chinzei, R., Watanabe, M., Shimizu-Saito, K., Hara, Y., Teramoto, K., Arii, S., Sato, C., Takase, K., Yasumizu, T., and Teraoka, H. (2003) Human umbilical cord blood as a source of transplantable hepatic progenitor cells. *Stem Cells* **21,** 217–227
18. Kollet, O., Shivtiel, S., Chen, Y. Q., Suriawinata, J., Thung, S. N., Dabeva, M. D., Kahn, J., Spiegel, A., Dar, A., Samira, S., *et al.* (2003) HGF, SDF-1, and MMP-9 are involved in stress-induced human CD34+ stem cell recruitment to the liver. *J. Clin. Invest.* **112,** 160–169
19. Newsome, P. N., Johannessen, I., Boyle, S., Dalakas, E., McAulay, K. A., Samuel, K., Rae, F., Forrester, L., Turner, M. L., Hayes, P. C., Harrison, D. J., Bickmore, W. A., and Plevris, J. N. (2003) Human cord blood-derived cells can differentiate into hepatocytes in the mouse liver with no evidence of cellular fusion. *Gastroenterology* **124,** 1891–1900
20. Nonome, K., Li, X. K., Takahara, T., Kitazawa, Y., Funeshima, N., Yata, Y., Xue, F., Kanayama, M., Shinno, E., Kuwae, C., Saito, S., Watanabe, A., and Sugiyama, T. (2005) Human umbilical cord blood-derived cells differentiate into hepatocyte-like cells in the Fas-mediated liver injury model. *Am. J. Physiol.* **289,** G1091–G1099
21. Sharma, A. D., Cantz, T., Richter, R., Eckert, K., Henschler, R., Wilkens, L., Jochheim-Richter, A., Arseniev, L., and Ott, M. (2005) Human cord blood stem cells generate human cytokeratin 18-negative hepatocyte-like cells in injured mouse liver. *Am. J. Pathol.* **167,** 555–564
22. Tanabe, Y., Tajima, F., Nakamura, Y., Shibasaki, E., Wakejima, M., Shimomura, T., Murai, R., Murawaki, Y., Hashiguchi, K., Kanbe, T., *et al.* (2004) Analyses to clarify rich fractions in hepatic progenitor cells from human umbilical cord blood and cell fusion. *Biochem. Biophys. Res. Commun.* **324,** 711–718
23. Wang, X., Ge, S., McNamara, G., Hao, Q. L., Crooks, G. M., and Nolta, J. A. (2003) Albumin-expressing hepatocyte-like cells develop in the livers of immune-deficient mice that received transplants of highly purified human hematopoietic stem cells. *Blood* **101,** 4201–4208
24. Ito, M., Hiramatsu, H., Kobayashi, K., Suzue, K., Kawahata, M., Hioki, K., Ueyama, Y., Koyanagi, Y., Sugamura, K., Tsuji, K., Heike, T., and Nakahata, T. (2002) NOD/SCID/gamma(c)(null) mouse: an excellent recipient mouse model for engraftment of human cells. *Blood* **100,** 3175–3182
25. Hiramatsu, H., Nishikomori, R., Heike, T., Ito, M., Kobayashi, K., Katamura, K., and Nakahata, T. (2003) Complete reconstitution of human lymphocytes from cord blood CD34+ cells using the NOD/SCID/gammacnull mice model. *Blood* **102,** 873–880
26. Kambe, N., Hiramatsu, H., Shimonaka, M., Fujino, H., Nishikomori, R., Heike, T., Ito, M., Kobayashi, K., Ueyama, Y., Matsuyoshi, N., Miyachi, Y., and Nakahata, T. (2004) Development of both human connective tissue-type and mucosal-type mast cells in mice from hematopoietic stem cells with identical distribution pattern to human body. *Blood* **103,** 860–867
27. Tomita, M., Yamamoto, K., Kobashi, H., Ohmoto, M., and Tsuji, T. (1994) Immunohistochemical phenotyping of liver macrophages in normal and diseased human liver. *Hepatology* **20,** 317–325
28. Cramer, T., Schuppan, D., Bauer, M., Pfander, D., Neuhaus, P., and Herbst, H. (2004) Hepatocyte growth factor and c-Met expression in rat and human liver fibrosis. *Liver. Int.* **24,** 335–344
29. Ljubimova, J. Y., Petrovic, L. M., Wilson, S. E., Geller, S. A., and Demetriou, A. A. (1997) Expression of HGF, its receptor c-met, c-myc, and albumin in cirrhotic and neoplastic human liver tissue. *J. Histochem. Cytochem.* **45,** 79–87
30. Selzner, N., Selzner, M., Odermatt, B., Tian, Y., Van Rooijen, N., and Clavien, P. A. (2003) ICAM-1 triggers liver regeneration through leukocyte recruitment and Kupffer cell-dependent release of TNF-alpha/IL-6 in mice. *Gastroenterology* **124,** 692–700
31. Manz, M. G., Miyamoto, T., Akashi, K., and Weissman, I. L. (2002) Prospective isolation of human clonogenic common myeloid progenitors. *Proc. Natl. Acad. Sci. U. S. A.* **99,** 11872–11877
32. Wang, X., Montini, E., Al-Dhalimy, M., Lagasse, E., Finegold, M., and Grompe, M. (2002) Kinetics of liver repopulation after bone marrow transplantation. *Am. J. Pathol.* **161,** 565–574

Received for publication March 24, 2006.
Accepted for publication May 10, 2007.

ELSEVIER

Cardiovascular Research 76 (2007) 119–131

Cardiovascular Research

www.elsevier.com/locate/cardiores

Flk1$^+$ cardiac stem/progenitor cells derived from embryonic stem cells improve cardiac function in a dilated cardiomyopathy mouse model

Shiro Baba[a,*], Toshio Heike[a], Momoko Yoshimoto[a], Katsutsugu Umeda[a], Hiraku Doi[a], Toru Iwasa[a], Xue Lin[b], Satoshi Matsuoka[c], Masashi Komeda[b], Tatsutoshi Nakahata[a]

[a] *Department of Pediatrics, Graduate School of Medicine, Kyoto University, Kyoto, Japan, 54 Kawahara-cho, Shogoin, Sakyo-ku, Kyoto 606-8507, Japan*
[b] *Department of Cardiovascular Surgery, Graduate School of Medicine, Kyoto University, Kyoto, Japan*
[c] *Department of Physiology and Biophysics, Graduate School of Medicine, Kyoto University, Kyoto, Japan*

Received 5 October 2006; received in revised form 2 May 2007; accepted 11 May 2007
Available online 17 May 2007
Time for primary review 18 days

Abstract

Objectives: Flk1$^+$ cells derived from embryonic stem (ES) cells are known to differentiate into mesodermal lineages such as hematopoietic and endothelial cells. Here we demonstrate that they can develop into cardiomyocytes that support functional recovery in a dilated cardiomyopathy (DCM) C57/BL6 mouse model.
Methods: Flk1$^+$ and Flk1$^-$ cells were sorted at day 4 of differentiation, and cardiomyogenesis was assessed in vitro. Next, we transplanted these cells into the hearts of cardiomyopathy mice to assess improvement in cardiac function.
Results: Flk1$^+$ cells, but not Flk1$^-$ cells, isolated on day 4 after differentiation were efficiently converted into contractile cardiomyocytes. RT-PCR analysis and immunohistological assays demonstrated that contractile cells derived from Flk1$^+$ cells in vitro expressed mature cardiac markers on day 10 after differentiation. Transplantation of sorted Flk1$^+$ cells into DCM model mouse hearts improved cardiac function, as determined by echocardiography and cardiac catheterization. The in vivo differentiated Flk1$^+$ cells expressed cardiac markers and had gap junctions, as demonstrated by immunohistochemistry. Furthermore, these cells generated ventricular type action potentials similar to those of adult ventricle.
Conclusion: These results indicate that Flk1 is a good marker for sorting cardiac stem/progenitor cells which can differentiate into mature cardiomyocytes both in vitro and in vivo.
© 2007 European Society of Cardiology. Published by Elsevier B.V. All rights reserved.

Keywords: Cell culture/isolation; Cell differentiation; Cell therapy; Cardiomyopathy

1. Introduction

At present, heart transplantation is the most frequently used and, indeed, the only effective therapy for end stage heart failure patients [1]. However, too few hearts are available for transplantation to meet demand.

To overcome this problem, work in recent years has attempted to develop cell transplantation protocols using various cell types. Although fetal cardiomyocytes [2] and skeletal muscle [3] are known candidates, it is not feasible to harvest fetal cardiomyocytes from human fetuses and skeletal muscle derived cells may promote life threatening arrhythmias because of a lack of gap junction formation between the transplanted cells and host cardiomyocytes [4,5]. Bone marrow is another candidate cell type [6]. However, while these cells can differentiate into vascular cells or induce angiogenesis, they very rarely differentiate into cardiomyocytes [7]. Thus, these previously considered cell types do not seem to be able to differentiate into cardiomyocytes efficiently.

Recently, embryonic stem (ES) cells and adult cardiac stem (CS) cells have been proposed as transplantable cell candidates that would avoid the problems described above [8–10]. With regard to CS cells, cardiomyocytes derived from adult CS cells in vivo have contractile capacity and bear gap junctions on their cell surface [10]. Although adult CS cells are good

* Corresponding author. Tel.: +81 75 751 3295; fax: +81 75 752 2361.
E-mail address: shibaba@kuhp.kyoto-u.ac.jp (S. Baba).

0008-6363/$ - see front matter © 2007 European Society of Cardiology. Published by Elsevier B.V. All rights reserved.
doi:10.1016/j.cardiores.2007.05.013

candidates for heart cell transplantation, it is hard to harvest these cells abundantly from the patient's own heart. With regard to ES cells, cardiomyogenesis from ES cells has been well studied in vitro [8,9]. However, procedure by which the ES cell progeny can be transplanted into the heart have not yet been established. Although Min et al. [11] did demonstrate improved cardiac function in post-infarcted rats upon transplantation with various cells, including mature cardiomyocytes derived from ES cells, it was difficult to purify the cardiomyocytes from this population by the hanging drop culture method. For heart cell transplantation, it is better to purify the transplanted cells as stem/progenitor cells that have the capacity to differentiate into cardiomyocytes. Therefore, a better transplantable cell candidate needs to be identified.

In this report, we identify cardiac stem/progenitor cells expressing Flk1, which is lateral mesodermal marker, and demonstrate that these cells effectively differentiate into cardiomyocytes both in vitro and in vivo. Transplantation of these cells into the hearts of dilated cardiomyopathy (DCM) model mice significantly improves their cardiac function.

2. Materials and methods

2.1. Cell lines, culture and differentiation

For these experiments, we used Gact4 mouse ES cells and which were maintained in the presence of 1% FCS, 10% Knockout-SR (GIBCO) and 5000 units/ml leukemia inhibitory factor (LIF) on 0.1% gelatin coated culture dishes as described [12]. The Gact4 cell line, which was produced by stable transfection with the enhanced GFP gene driven by the CAG promoter (a kind gift from Dr. Ogawa). Gact4 cells were differentiated as described previously [13]. Briefly, single cell dispersions of undifferentiated Gact4 cells were suspended in MEM Alpha medium (GIBCO) containing 10% FCS (EQUITECH BIO Inc.) and 5×10^{-5}M 2-mercaptoethanol in the absence of LIF (differentiation medium) at an initial concentration of 1.2×10^5 cells on 100 mm type IV collagen-coated culture dishes (Becton Dickinson).

2.2. FACS and comparison of Flk1+ and Flk1− cell differentiation into cardiomyocytes, endothelial colonies, and blood clusters in vitro

After 4 days of differentiation, Gact4 ES cells were dissociated into single cells by using Cell Dissociation Buffer (GIBCO), and separated Gact4 cells were labeled with an APC-conjugated AVAS12 antibody (anti-Flk1) [13] and sorted into $Flk1^+$ and $Flk1^-$ cells using a FACS Vantage SE (BD Biosciences). Each cell type was co-cultured in differentiation medium without cytokines at 500 cells per well in 24-well plates (FALCON) on OP-9 stromal cells, which were kindly provided by Dr. Kodama and maintained as described previously [14]. These 4 days-differentiated Gact4 cells were also characterized using a PE-conjugated anti-mouse Sca-1 antibody and a PE-conjugated anti-mouse c-kit antibody (BD Biosciences). The number of contractile colonies in each 24-well plate was counted. Endothelial colonies were characterized by a sheet-like structure that stained with DiI-acetylated low-density lipoprotein (DiI-Ac-LDL) (Molecular Probes) [15] and were also counted. Hematopoietic clusters were characterized by their cobblestone appearance [16]. Sorted cells were incubated in differentiation medium on OP-9 stromal cells as described above, and, after 24 h, the medium was replaced with fresh semisolid medium containing 10% fetal calf serum (EQUITECH BIO Inc.) and 1.2% methylcellulose (Shinetsu Chemical) without cytokines. The number of hematopoietic clusters on the 24-well plates were then counted as described previously [16].

2.3. Immunohistochemistry

Cells and 7 μm tissue slices were fixed with 4% paraformaldehyde and incubated with antibodies specific for the following markers: myosin light chain 2v (MLC2v) (Alexis Biochemicals, Inc.), atrial natriuretic peptide (ANP) (Protos Biotech Corporation), sarcomeric protein MF20 (MF20) (Hybridoma bank), sarcomeric protein CH1 (CH1) (Sigma), cardiac troponin-I (cTn-I) (Santa Cruz Biotechnology), connexin 43 (Cx43) (Zymed Laboratories, Inc.), CD45 (Becton Dickinson), CD31 (Becton Dickinson), skeletal myosin heavy chain (MHC) (Zymed Laboratories, Inc.), mouse Ki-67 (Dako Cytomation) and GFP (Nacalai tesque). Peroxidase- or Cy3-conjugated donkey anti-mouse IgG, Alkaline phosphatase (ALP)- or Cy3-conjugated donkey anti-rabbit IgG, ALP- or Cy3-conjugated donkey anti-goat IgG, and peroxidase- or Cy3-conjugated goat anti-rat IgG (Jackson ImmunoResearch Laboratories, Inc.) served as secondary antibodies. ALP- or peroxidase-conjugated cells were visualized by using the Alkaline Phosphatase Substrate Kit III or the DAB Substrate Kit (Vector Laboratories, Inc.). All heart sections were incubated with these antibodies using the M.O.M. kit (Vector Laboratories, Inc.) to prevent non-specific reactions. Many heart slices were also stained with hematoxylin-eosin (HE) to detect abnormal cell growth due to transplanted $Flk1^+$ or $Flk1^-$ cells.

2.4. RT-PCR analysis

PCR amplifications used the primers described in Table 1. The PCR conditions for all primers were DNA denaturation at 94 °C for 5 min, 25–30 cycles of 94 °C for 30 s, 60 °C for 30 s, and 72 °C for 60 s, followed by a final extension step at 72 °C for 7 min.

2.5. Electrophysiological examination in vitro

Day 4-sorted $Flk1^+$ Gact4 ES cells were co-cultured with OP-9 stromal cells on MED-probe dishes (ALPHA MED SCIENCES) and the electrical potentials of contractile colonies derived from these cells were recorded by using

Table 1
PCR primers

Flk1	Forward	5′-TAAAAGCAGGGAGTCTGTGG-3′
	Reverse	5′-ATCTAAGCAGCACCTCTCTC-3′
GATA-4	Forward	5′-CTCGATATGTTTGATGACTTCT-3′
	Reverse	5′-CGTTTTCTGGTTTGAATCCC-3′
Nkx2.5	Forward	5′-GTGGGTCTCAATGCCTATG-3′
	Reverse	5′-CTCTTTCCCTACCAGGCTC-3′
MLC2v	Forward	5′-GCCAAGAAGCGGATAGAAGG-3′
	Reverse	5′-CTGTGGTTCAGGGCTCAGTC-3′
MLC2a	Forward	5′′-CAGACCTGAAGGAGACCT-3′
	Reverse	5′-GTCAGCGTAAACAGTTGC-3′
Cx43	Forward	5′-TGGGGGAAAGGCGTGAG-3′
	Reverse	5′-CTGCTGGCTCTGCTGGAAGGT-3′
Nanog	Forward	5′-GTTTGCCTAGTTCTGAGGAAGCA-3′
	Reverse	5′-CTGCTGGAGGCTGAGGTACTTCT-3′
Oct4	Forward	5′-GGCGTTCTCTTTGGAAAGGTG-3′
	Reverse	5′-CTCGAACCACATCCTTCTCT-3′
GAPDH	Forward	5′-TCCAGAGGGGCCATCCACAGTC-3′
	Reverse	5′-GTCGGTGTGAACGGATTTGGCC-3′

the MED64 System (Panasonic multi-electrode system; ALPHA MED SCIENCES).

2.6. Transplantation of ES cells to doxorubicin-induced DCM model mice

To produce DCM model mice, we used 8 wk-old male C57/BL6 mice. The MHC types of this mouse and Gact4 cells are very similar. The MHC H2 haplotypes of Gact4 and C57/BL6 are both type b. All animal handling procedures followed the Guide for the Care and Use of Laboratory Animals published by the US National Institutes of Health (NIH Publication No. 85–23, revised 1996) and the guidelines of the Animal Research Committee of the Graduate School of Medicine, Kyoto University. We injected a 3 mg/kg dose of doxorubicin intraperitoneally (i.p.) 6 times over 2 weeks. Four weeks after the last i.p. injection, mice that had a left ventricular diastolic diameter (LVDd) larger than 3.8 mm or 120% of the LVDd before the injections were used as the DCM models in these experiments. Cell transplantation was performed 4 wks after the final i.p. injection with doxorubicin. Mice were intubated and connected to a ventilator (MiniVent, Type845) (Hugo Sachs Elektronik, Germany), and cell transplantation was performed under anesthesia with 1.0–1.5% Sevoflurane (Maruishi Seiyaku). A freshly harvested 10 μl $Flk1^+$ cell suspension (3×10^5/10 μl) was directly injected into a site on the anterior-lateral wall of the left ventricle. Medium-treated mice were injected with the equivalent volume of cell-free medium. Similarly, a freshly 10 μl harvested $Flk1^-$ cell suspension (3×10^5/10 μl) was injected into nine DCM model mice.

2.7. Hemodynamic measurements and electrocardiogram recordings

Hemodynamics were indirectly measured via echocardiography with a 15 to 16 MHz phased-array transducer (model 21390A, PHILIPS). LVDd and left ventricular systolic diameter (LVDs) were measured and the left ventricular ejection fraction (LVEF) was calculated as described [6]. Cardiac catheterization was performed four weeks after cell transplantation, as described [17], using a 1.4-Fr micromenometer-tipped catheter (Miller Instruments Inc.), a pressure transducer (model TCB-500, MILLER INSTRUMENT INC.) and a chart-strip recorder (Thermal Array Recorder, model RTA-1100M) (NIHON KOHDEN). Left ventricular maximum systolic velocity (+ dP/dt) and minimum diastolic velocity (− dP/dt) were calculated from the left ventricular pressure curve. Limb-lead electrocardiograpm was recorded by a PowerLab System (PowerLab 4/25 ML845 and BIO Amp CF ML132) (ADInstruments). All measurements were performed under anesthesia with mask inhalation of 0.5–1.0% Sevoflurane and a heart rate of approximately 450/min.

2.8. FISH analysis

FISH analysis was performed on 20 μm tissue sections fixed with 4% paraformaldehyde according to the method described previously [18]. We used a DIG-labeled GFP probe [18] and a Biotin-labeled mouse chromosome Y specific probe (Cambio Ltd). The DIG-labeled GFP probe was visualized with rabbit anti-DIG/HRPDIG (Dako Cytomation) and the TSA Fluorescein System (PerkinElmer Life Sciences), and the Biotin-labeled mouse chromosome Y probe was visualized with Cy3-conjugated streptavidin (Jackson ImmunoResearch Laboratories, Inc.) on a fluorescence microscope (Leica, LEICA DM 6000B). Finally, nuclei were counterstained with Hoechst33342. The figures were subjected to computer graphics analysis. The nuclei in the sample were dissected from top to bottom with a thickness of 1 μm. We confirmed that a complete observation of the nucleus had been achieved.

2.9. Isolation of single cells and action potential measurements

Ventricular myocytes were dissociated from mouse hearts by perfusing collagenase (Worthington Biochemical Corporation), protease (Sigma–Aldrich,), and trypsin (Sigma–Aldrich,) in essentially the same method as described previously [19]. GFP^+ cardiomyocytes were identified on a fluorescence microscope and the membrane potential was recorded by the current-clamp and perforated patch techniques (0.3 mmol/L amphotericin B) using a patch clamp amplifier (Axopatch 200B, Axon Instruments, Inc.) in a control Tyrode solution (140 mM NaCl, 5.4 mM KCl, 1.8 mM $CaCl_2$, 0.5 mM $MgCl_2$, 0.3 mM NaH_2PO_4, 5.5 mM glucose and 5.0 mM HEPES, pH=7.4 with NaOH) at 36–37 °C.

2.10. Ectopic transplantation

A freshly harvested 10 μl $Flk1^+$ cell suspension (3×10^5/10 μl) was injected subcutaneously into the backs of five

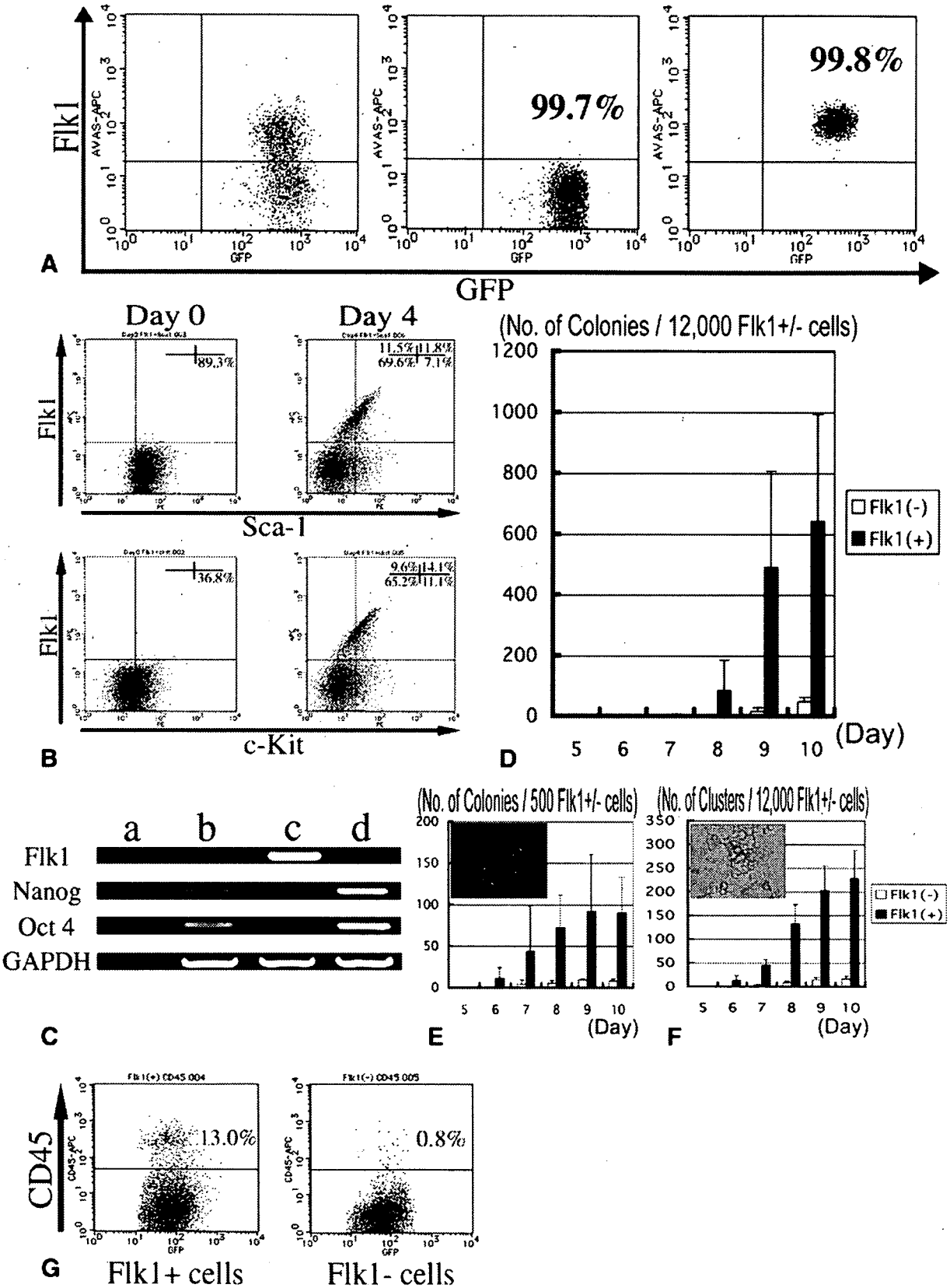
A
Flk1
AVAS-APC
GFP
99.7%
99.8%
B
Day 0
Day 4
Flk1
Sca-1
c-Kit
89.3%
36.8%
11.5%
11.8%
69.6%
7.1%
9.6%
14.1%
65.2%
11.1%
C
a
b
c
d
Flk1
Nanog
Oct 4
GAPDH
D
(No. of Colonies / 12,000 Flk1+/- cells)
Flk1(-)
Flk1(+)
(Day)
E
(No. of Colonies / 500 Flk1+/- cells)
F
(No. of Clusters / 12,000 Flk1+/- cells)
G
CD45
13.0%
0.8%
Flk1+ cells
Flk1- cells

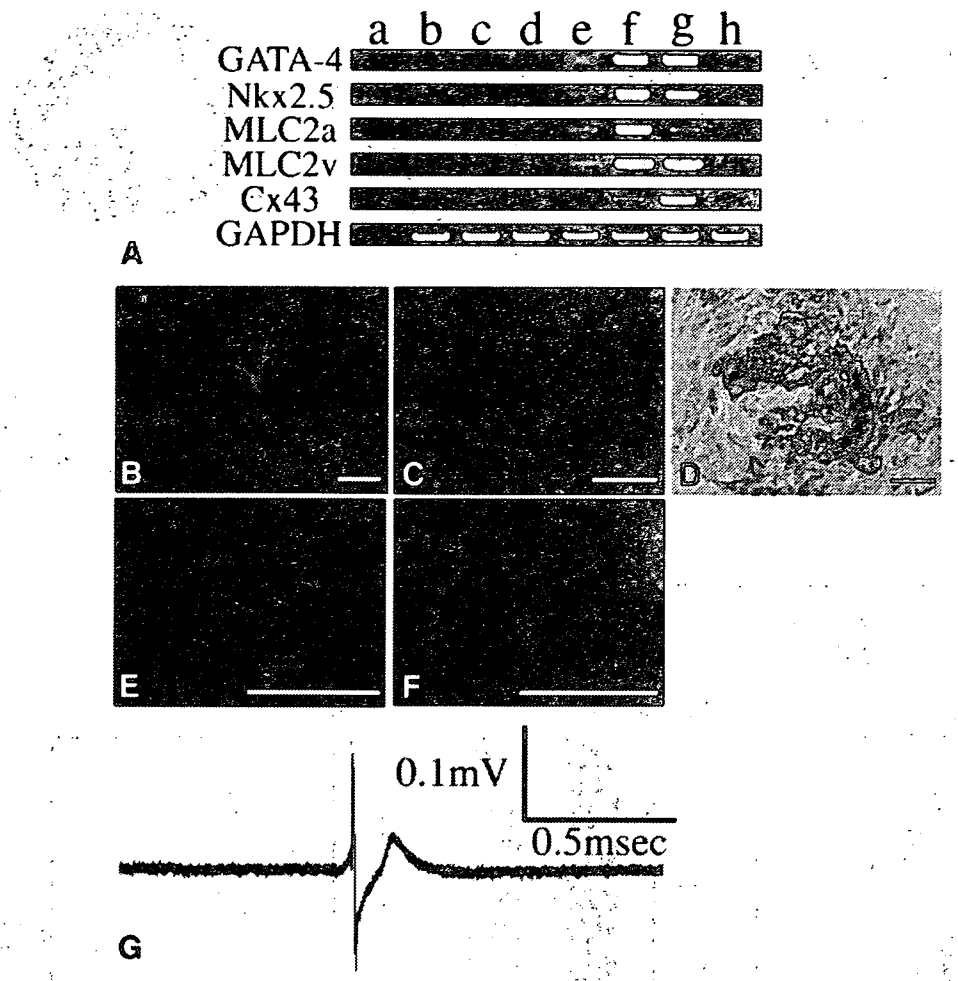

Fig. 2. Flk1$^+$ cells were assessed for expression of various cardiac markers by RT-PCR and immunohistochemistry. (A) RT-PCR to detect the cardiac markers GATA-4, Nkx2.5, MLC2a, MLC2v and Cx43. Lane (a) shows the RT-PCR control, where water replaced the cellular mRNA, lanes (b–h) show the RT-PCR using mRNA from undifferentiated ES cells (b), Flk1$^-$ cells (c), Flk1$^+$ cells (d), Flk1$^-$ cell-derived contractile colonies at differentiation day 10 (e), Flk1$^+$ cell-derived contractile colonies at differentiation day 10 (f), mouse ventricular cells (g), and OP-9 stromal cells (h). (B–F) In the immunohistochemical analysis, contractile colonies were stained for MLC2v (B), ANP (C), MF20 (E) and cTn-I (F). In (D), the colonies were double stained for MLC2v (brown) and ANP (blue). Bar, 100 μm. (G) Electrical activities were measured from contractile colonies.

mice and kidney capsules of five mice at 14 weeks of age. Tissues from these areas were removed four and ten weeks after transplantation.

2.11. Statistical analysis

Data were statistically analyzed using a two-tailed unpaired *t*-test within Microsoft Excel. Statistical significance was defined as $p<0.05$.

3. Results

3.1. Flk1+ cells differentiate into cardiomyocytes, endothelial cells and hematopoietic cells more frequently than Flk1− cells

We sorted differentiated ES cells into Flk1$^+$ and Flk1$^-$ cells after 4 days of culture in differentiation medium (Fig. 1A), and evaluated their differentiation potentials at days 5–10 after differentiation. On day 4 after differentiation,

Fig. 1. Differentiation potential of sorted day 4-Flk1$^+$ and Flk1$^-$ cells. On day 4 of Gact4 ES cell culture, the Flk1$^+$ and Flk1$^-$ cells were sorted using an AVAS12(Flk1)-APC antibody for FACS (A) and characterized with Sca-1 and c-kit antibodies by FACS (B). (C) Nanog and Oct4 expressions in Flk1$^+$ and Flk1$^-$ cells. Lane (a) shows the RT-PCR control, where water replaced the cellular mRNA, lanes (b–d) show the RT-PCR products from Flk1$^-$ cells (b), Flk1$^+$ cells (c), and undifferentiated mouse ES cells (d). The contractile colonies (D), endothelial colonies (E), and hematopoietic clusters (F) that were generated from Flk1$^+$ or Flk1$^-$ cells were counted on the indicated days after differentiation. Black bars and open bars indicate the number of colonies derived from Flk1$^+$ and Flk1$^-$ cells, respectively. In (E) and (F), the insets show a sheet-like DiI-Ac-LDL-stained endothelial colony and the in situ appearance of a hematopoietic cluster, respectively. (G) FACS analysis of the CD45 expression of hematopoietic cells derived from Flk1$^+$ and Flk1$^-$ cells on day 10 of differentiation.